

Precision Neutrino Oscillation Physics with an Intermediate Baseline Reactor Neutrino Experiment

Sandhya Choubey^{1,2}, S.T. Petcov^{2,1,3}, and M. Piai⁴

¹*INFN, Sezione di Trieste, Trieste, Italy*

²*Scuola Internazionale Superiore di Studi Avanzati, I-34014 Trieste, Italy*

³*Institute of Nuclear Research and Nuclear Energy,*

Bulgarian Academy of Sciences, 1784 Sofia, Bulgaria and

⁴*Department of Physics, Yale University, New Haven CT 06520 USA*

We discuss the physics potential of intermediate $L \sim 20 \div 30$ km baseline experiments at reactor facilities, assuming that the solar neutrino oscillation parameters Δm_{\odot}^2 and θ_{\odot} lie in the high-LMA solution region. We show that such an intermediate baseline reactor experiment can determine both Δm_{\odot}^2 and θ_{\odot} with a remarkably high precision. We perform also a detailed study of the sensitivity of the indicated experiment to Δm_{atm}^2 , which drives the dominant atmospheric ν_{μ} ($\bar{\nu}_{\mu}$) oscillations, and to θ - the neutrino mixing angle limited by the data from the CHOOZ and Palo Verde experiments. We find that this experiment can improve the bounds on $\sin^2 \theta$. If the value of $\sin^2 \theta$ is large enough, $\sin^2 \theta \gtrsim 0.02$, the energy resolution of the detector is sufficiently good and if the statistics is relatively high, it can determine with extremely high precision the value of Δm_{atm}^2 . We also explore the potential of the intermediate baseline reactor neutrino experiment for determining the type of the neutrino mass spectrum, which can be with normal or inverted hierarchy. We show that the conditions under which the type of neutrino mass hierarchy can be determined are quite challenging, but are within the reach of the experiment under discussion.

PACS numbers: 14.60.Pq 13.15.+g

I. INTRODUCTION

The experiments with solar, atmospheric and reactor neutrinos [1, 2, 3, 4, 5, 6] have provided in recent years remarkable evidences for the existence of neutrino oscillations driven by nonzero neutrino masses and neutrino mixing. The hypothesis of solar neutrino oscillations, which in one variety or another were considered as the most natural explanation of the solar neutrino deficit [1, 2] since the late 60'ies (see, e.g., [7, 8, 9]), has received a convincing confirmation from the measurement of the solar neutrino flux through the neutral current reaction on deuterium by the SNO experiment [3]. The analysis of the solar neutrino data obtained by Homestake, SAGE, GALLEX/GNO, SK and SNO experiments showed that the data favor the Large Mixing Angle (LMA) MSW solution with the two-neutrino oscillation parameters - the solar neutrino mixing angle and the mass squared difference, lying at 99.73% C.L. in the region [3, 10]:

$$3 \times 10^{-5} \text{eV}^2 \lesssim \Delta m_{\odot}^2 \lesssim 3.5 \times 10^{-4} \text{eV}^2 \quad (1)$$

$$0.21 \lesssim \sin^2 \theta_{\odot} \lesssim 0.47. \quad (2)$$

The first results of the KamLAND reactor experiment [6] has confirmed, under the plausible assumption of CPT-invariance which we will suppose to hold throughout this study, the LMA MSW solution, establishing it essentially as a unique solution of the solar neutrino problem. The combined fits to the available solar neutrino and KamLAND data, performed by several collaborations within the two-neutrino mixing hypothesis, identify two distinct solution sub-regions within the LMA solution region [11, 12, 13]. Adding the KamLAND data did not lead to a considerable reduction of the interval of allowed values of $\sin^2 \theta_{\odot}$ with respect to the one quoted in eq. (1), while the best fit values of Δm_{\odot}^2 in the two sub-regions (labeled from now on low-LMA and high-LMA) are given by [12]:

$$\text{low-LMA: } \Delta m_{\odot}^2 \simeq 7.2 \times 10^{-5} \text{eV}^2, \quad (3)$$

$$\text{high-LMA: } \Delta m_{\odot}^2 \simeq 1.5 \times 10^{-4} \text{eV}^2. \quad (4)$$

The observed Zenith angle dependence of the multi-GeV μ -like events in the Super-Kamiokande experiment unambiguously demonstrated the disappearance of the atmospheric ν_{μ} ($\bar{\nu}_{\mu}$) on distances $L \gtrsim 1000$ km. The Super-Kamiokande (SK) atmospheric neutrino data is best described, as is well-known, in terms of dominant $\nu_{\mu} \rightarrow \nu_{\tau}$ ($\bar{\nu}_{\mu} \rightarrow$

$\bar{\nu}_\tau$) oscillations with (almost) maximal mixing and neutrino mass squared difference of $|\Delta m_{\text{atm}}^2| \cong (1.4 - 5.0) \times 10^{-3} \text{ eV}^2$ (99.73% C.L.) [4]. According to the more recent combined analysis of the data from the SK and K2K experiments [14] one has at 99.73% C.L.:

$$1.5 \times 10^{-3} \text{ eV}^2 \lesssim |\Delta m_{\text{atm}}^2| \lesssim 3.7 \times 10^{-3} \text{ eV}^2 \quad (5)$$

The neutrino oscillation description of the combined solar and atmospheric neutrino data requires the existence of three-neutrino mixing in the weak charged lepton current (see, e.g., [15]):

$$\nu_{lL} = \sum_{j=1}^3 U_{lj} \nu_{jL}. \quad (6)$$

Here ν_{lL} , $l = e, \mu, \tau$, are the three left-handed flavor neutrino fields, ν_{jL} is the left-handed field of the neutrino ν_j having a mass m_j and U is the Pontecorvo-Maki-Nakagawa-Sakata (PMNS) neutrino mixing matrix [16, 17]. The PMNS mixing matrix U can be parameterized by three angles, θ_{atm} , θ_{\odot} , and θ , and, depending on whether the massive neutrinos ν_j are Dirac or Majorana particles - by one or three CP-violating phases [18, 19]. In the standard parameterization of U (see, e.g., [15]) the three mixing angles are denoted as θ_{12} , θ_{13} and θ_{23} :

$$U = \begin{pmatrix} U_{e1} & U_{e2} & U_{e3} \\ U_{\mu 1} & U_{\mu 2} & U_{\mu 3} \\ U_{\tau 1} & U_{\tau 2} & U_{\tau 3} \end{pmatrix} = \begin{pmatrix} c_{12}c_{13} & s_{12}c_{13} & s_{13}e^{-i\delta} \\ -s_{12}c_{23} - c_{12}s_{23}s_{13}e^{i\delta} & c_{12}c_{23} - s_{12}s_{23}s_{13}e^{i\delta} & s_{23}c_{13} \\ s_{12}s_{23} - c_{12}c_{23}s_{13}e^{i\delta} & -c_{12}s_{23} - s_{12}c_{23}s_{13}e^{i\delta} & c_{23}c_{13} \end{pmatrix} \quad (7)$$

where we have used the usual notations, $s_{ij} \equiv \sin \theta_{ij}$, $c_{ij} \equiv \cos \theta_{ij}$, and δ is the Dirac CP-violation phase¹. If we identify the two independent neutrino mass squared differences in this case, Δm_{21}^2 and Δm_{31}^2 , with the neutrino mass squared differences which drive the solar and atmospheric neutrino oscillations, $\Delta m_{\odot}^2 = \Delta m_{21}^2 > 0$, $\Delta m_{\text{atm}}^2 = \Delta m_{31}^2$, one has: $\theta_{12} = \theta_{\odot}$, $\theta_{23} = \theta_{\text{atm}}$, and $\theta_{13} = \theta$.

The angle θ is limited by the data from the CHOOZ and Palo Verde experiments [21, 22] which searched for evidences for oscillations of reactor $\bar{\nu}_e$ at ~ 1 km from the source. No disappearance of $\bar{\nu}_e$ was observed. In a two-neutrino oscillation analysis performed in [21] a stringent upper bound on the value of θ in the region of $|\Delta m^2| \geq 1.5 \times 10^{-3} \text{ eV}^2$ was obtained. A 3- ν oscillation analysis of the CHOOZ data² [23] led to the conclusion that for $\Delta m_{\odot}^2 \lesssim 10^{-4} \text{ eV}^2$, the limits on $\sin^2 \theta$ practically coincide with those derived in the 2- ν oscillation analysis in [21]. A combined 3- ν oscillation analysis of the solar neutrino, CHOOZ and the KamLAND data, performed under the assumption of $\Delta m_{\odot}^2 \ll |\Delta m_{\text{atm}}^2|$ (see, e.g., [15, 24]), showed that [11]

$$\sin^2 \theta < 0.05, \quad 99.73\% \text{ C.L.} \quad (8)$$

The precise upper limit in Eq. (8) is Δm_{atm}^2 -dependent. The authors of [11] found the best-fit value of $\sin^2 \theta$ to lie in the interval³ $\sin^2 \theta \cong (0.00 - 0.01)$.

Somewhat better limits on $\sin^2 \theta$ than the existing one can be obtained in the MINOS experiment [26]. Various options are being currently discussed (experiments with off-axis neutrino beams, more precise reactor antineutrino and long baseline experiments, etc., see, e.g., [27]) of how to improve by at least an order of magnitude, i.e., to values of ~ 0.005 or smaller, the sensitivity to $\sin^2 \theta$.

Let us note that the atmospheric neutrino and K2K data do not allow one to determine the sign of Δm_{atm}^2 . This implies that if we identify Δm_{atm}^2 with Δm_{31}^2 in the case of 3-neutrino mixing, one can have $\Delta m_{31}^2 > 0$ or $\Delta m_{31}^2 < 0$. The two possibilities correspond to two different types of neutrino mass spectrum: with normal hierarchy (NH), $m_1 < m_2 < m_3$, and with inverted hierarchy (IH), $m_3 < m_1 < m_2$.

After the spectacular experimental progress made in the last two years or so in the studies of neutrino oscillations, further understanding, in particular, of the structure of the neutrino masses and mixing, of their origins and of the status of the CP-symmetry in the lepton sector requires a large and challenging program of high precision measurements to be pursued in neutrino physics. One of the first goals of this program is to improve the precision

¹ We have not written explicitly the two possible Majorana CP-violation phases [18, 19] which do not enter into the expressions for the oscillation probabilities of interest [18, 20]. We assume throughout this study $0 \leq \theta_{12}, \theta_{23}, \theta_{13} < \pi/2$.

² In this case $\Delta m^2 = \Delta m_{\text{atm}}^2$.

³ The possibility of large $\sin^2 \theta > 0.97$, which is admitted by the CHOOZ data alone, is incompatible with the neutrino oscillation interpretation of the solar neutrino data (see, e.g., [25]).

in the measurement of the mass squared differences and mixing angles which control the solar and the dominant atmospheric neutrino oscillations: Δm_{\odot}^2 , θ_{\odot} , and Δm_{atm}^2 , θ_{atm} . A step of fundamental importance would be the detection and the studies of sub-leading neutrino oscillation effects, if the latter are observable. This includes the measurement of, or getting more stringent upper limit on, the value of the third and the only small mixing angle in the PMNS matrix U , θ ($= \theta_{13}$), the exploration of the possible CP-violating effects and the determination of the type of the neutrino mass spectrum which can be with normal hierarchy (NH) or inverted hierarchy (IH). Among the further fundamental open questions, which cannot be answered by studying neutrino oscillations, but the progress in the studies of which requires a precise knowledge of the neutrino oscillation parameters, are i) the nature —Dirac or Majorana— of the massive neutrinos, ii) the absolute scale of neutrino masses, iii) the mechanism giving rise to the neutrino masses and mixing, iv) the possible relation between CP-violation in the lepton sector at low energies and the generation of the baryon asymmetry of the Universe by the leptogenesis mechanism, v) lepton number violation and its possible manifestation in charged lepton flavor violating decays, to name a few.

In the present article we explore the possibility of performing a high precision measurement of some of the 3-neutrino oscillation parameters in an intermediate baseline, $L \sim 20 \div 30$ km, reactor neutrino experiment. We first address the issue of precision determination of the solar neutrino oscillation parameters, Δm_{\odot}^2 and θ_{\odot} . The KamLAND experiment, as discussed by several authors [28], has a remarkable sensitivity to Δm_{\odot}^2 in the low-LMA region. However, the sensitivity of KamLAND to the value of θ_{\odot} is not found to be equally good. Even under the most optimistic conditions KamLAND is not expected to substantially reduce the region of allowed values of θ_{\odot} obtained from the analysis of the solar neutrino data [29]. The best conditions for precise determination of θ_{\odot} is in a reactor experimental set-up, where the baseline is tuned to a Survival Probability MINimum (SPMIN)⁴. With a baseline of about $L \sim 160$ km and $\Delta m_{\odot}^2 \sim 7.2 \times 10^{-5}$ eV² or 1.5×10^{-4} eV², KamLAND is essentially sensitive to a Survival Probability MAXimum (SPMAX). The sensitivity to SPMAX gives KamLAND the ability to determine Δm_{\odot}^2 with a high precision through the measurement of the distortion of the final state e^+ -spectrum, provided $\Delta m_{\odot}^2 < 2 \times 10^{-4}$ eV². At the same time it reduces KamLAND's sensitivity to the solar neutrino mixing angle [29]. As was shown in [29], a 70 km baseline reactor experiment could determine the solar neutrino mixing angle $\sin^2 \theta_{\odot}$ ($\tan^2 \theta_{\odot}$) to within 9.6 (14)% at the 99% C.L. in the case of the low-LMA solution of the solar neutrino problem. KamLAND essentially loses sensitivity to Δm_{\odot}^2 for $\Delta m_{\odot}^2 \gtrsim 2 \times 10^{-4}$ eV². Nevertheless, the more precise measurement of the spectrum of the final state e^+ in the KamLAND experiment is expected to unambiguously determine whether Δm_{\odot}^2 lies in the low-LMA or high-LMA region.

In this paper, following a previous suggestion and analysis in [30] (see also [31]), in the context of three neutrino mixing, we discuss the physics potential of intermediate $L \sim 20 \div 30$ km baseline experiments at reactor facilities. We show that such an intermediate baseline reactor experiment can determine both Δm_{\odot}^2 and θ_{\odot} with a remarkably high precision *if the solution of the solar neutrino problem is the high-LMA solution*. We perform also a detailed study of the sensitivity of the indicated experiment to the parameters Δm_{atm}^2 and $\sin^2 \theta$. We show that if the energy resolution of the detector is sufficiently good and if the statistics is relatively high, one can choose small enough energy bins so that even an experiment with an intermediate baseline of 20–30 km can be sensitive to the Δm_{atm}^2 driven oscillations. We find that this experiment can certainly improve the bounds on $\sin^2 \theta$ and if the value of $\sin^2 \theta$ is large enough, it can determine with extremely high precision the value of Δm_{atm}^2 .

We finally explore the potential of the intermediate baseline reactor neutrino experiment for determining the type of the neutrino mass spectrum which can be with normal or inverted hierarchy. The knowledge of the neutrino mass hierarchy is of crucial importance, in particular, for modeling of the neutrino mass matrix and understanding of the underlying physics of neutrino mass generation. The type of the neutrino mass hierarchy has been also shown to be an important “parameter” in a number of neutrino mixing and neutrino oscillation observables, such as the effective Majorana mass in neutrinoless double- β decay [32]. The neutrino mass hierarchy (or, e.g., the sign of Δm_{atm}^2) can be determined in very long baseline neutrino oscillation experiments at neutrino factories (see, e.g., [33]), and, e.g. using combined data from the long baseline oscillation experiments JHF-SK and NuMI with off-axis neutrino beams [34]. It was suggested in [30] that the “interference” effects between the Δm_{\odot}^2 and Δm_{atm}^2 driven oscillations can be used in reactor experiments to answer the question about the neutrino mass hierarchy. We show that the conditions under which the type of neutrino mass hierarchy can be determined are rather challenging, but are not out of reach of the experiment under discussion, provided the solar neutrino oscillation parameters lie in the high-LMA solution region.

⁴ A detailed discussion of SPMAX and SPMIN as well as θ_{\odot} sensitivity of the current and future experiments can be found in [29] and we do not repeat it here.

The expression for the $\bar{\nu}_e$ survival probability in the case of 3 flavor neutrino mixing and neutrino mass spectrum with normal hierarchy (NH) is given by ⁵ [23, 30, 35]:

$$\begin{aligned}
 P_{NH}(\bar{\nu}_e \rightarrow \bar{\nu}_e) &= 1 - 2 \sin^2 \theta \cos^2 \theta \left(1 - \cos \frac{\Delta m_{\text{atm}}^2 L}{2 E_\nu} \right) \\
 &- \frac{1}{2} \cos^4 \theta \sin^2 2\theta_\odot \left(1 - \cos \frac{\Delta m_\odot^2 L}{2 E_\nu} \right) \\
 &+ 2 \sin^2 \theta \cos^2 \theta \sin^2 \theta_\odot \left(\cos \left(\frac{\Delta m_{\text{atm}}^2 L}{2 E_\nu} - \frac{\Delta m_\odot^2 L}{2 E_\nu} \right) - \cos \frac{\Delta m_{\text{atm}}^2 L}{2 E_\nu} \right),
 \end{aligned} \tag{9}$$

where E_ν is the $\bar{\nu}_e$ energy. If the neutrino mass spectrum is with inverted hierarchy (IH), the $\bar{\nu}_e$ survival probability can be written in the form [23, 30, 35]:

$$\begin{aligned}
 P_{IH}(\bar{\nu}_e \rightarrow \bar{\nu}_e) &= 1 - 2 \sin^2 \theta \cos^2 \theta \left(1 - \cos \frac{\Delta m_{\text{atm}}^2 L}{2 E_\nu} \right) \\
 &- \frac{1}{2} \cos^4 \theta \sin^2 2\theta_\odot \left(1 - \cos \frac{\Delta m_\odot^2 L}{2 E_\nu} \right) \\
 &+ 2 \sin^2 \theta \cos^2 \theta \cos^2 \theta_\odot \left(\cos \left(\frac{\Delta m_{\text{atm}}^2 L}{2 E_\nu} - \frac{\Delta m_\odot^2 L}{2 E_\nu} \right) - \cos \frac{\Delta m_{\text{atm}}^2 L}{2 E_\nu} \right).
 \end{aligned} \tag{10}$$

The $\bar{\nu}_e$ survival probability does not depend either on the angle θ_{atm} associated with the atmospheric neutrino oscillations, nor on the CP violating phase δ in the PMNS matrix.

In the convention (we will call A) in which the neutrino masses are not ordered in magnitude and the NH neutrino mass spectrum corresponds to $m_1 < m_2 < m_3$, while the IH spectrum is associated with the ordering $m_3 < m_1 < m_2$, it is natural to choose

$$\Delta m_\odot^2 = \Delta m_{21}^2 > 0, \quad \text{Convention A.} \tag{11}$$

We can identify further Δm_{atm}^2 with Δm_{31}^2 in the case of NH spectrum,

$$\Delta m_{\text{atm}}^2 = \Delta m_{31}^2 > 0, \quad \text{NH spectrum (A),} \tag{12}$$

and with $\Delta m_{23}^2 > 0$ if the spectrum is of the IH type,

$$\Delta m_{\text{atm}}^2 = \Delta m_{23}^2 > 0, \quad \text{IH spectrum (A).} \tag{13}$$

In this convention the mixing angles in the standard parameterization of the PMNS mixing matrix U are given by:

$$\theta_{12} = \theta_\odot, \quad \theta_{23} = \theta_{\text{atm}}, \quad \theta_{13} = \theta, \quad \text{Convention A.} \tag{14}$$

One can also number (without loss of generality) the neutrinos with definite mass in vacuum ν_j in such a way that their masses obey $m_1 < m_2 < m_3$. In this alternative convention (we will denote as B) it is convenient to choose

$$\Delta m_{\text{atm}}^2 = \Delta m_{31}^2 > 0, \quad \text{Convention B.} \tag{15}$$

⁵ The Earth matter effects are negligible for the values of the neutrino oscillation parameters (Δm_\odot^2 and Δm_{atm}^2), $\bar{\nu}_e$ energies and the short baseline $L \simeq 20 \div 30$ km we are interested in.

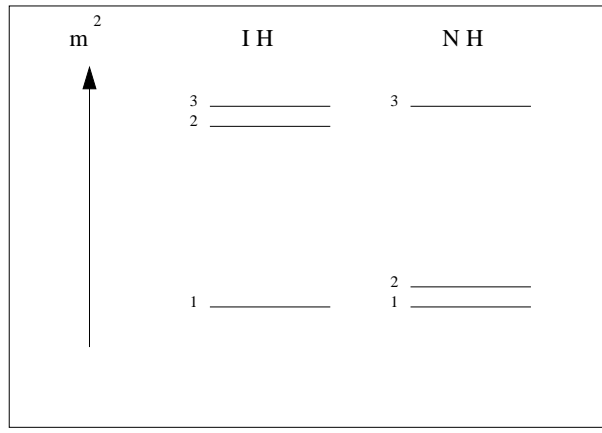


FIG. 1: The two possible neutrino mass spectra, with Normal Hierarchy (NH) and Inverted Hierarchy (IH), in the convention in which $m_1 < m_2 < m_3$ (convention B).

In the case of NH neutrino mass spectrum we have

$$\Delta m_{\odot}^2 = \Delta m_{21}^2 > 0, \quad \text{NH spectrum (B)}, \quad (16)$$

and

$$\theta_{12} = \theta_{\odot}, \quad \theta_{23} = \theta_{\text{atm}}, \quad \theta_{13} = \theta, \quad \text{NH spectrum (B)}, \quad (17)$$

where θ_{ij} are the angles in the standard parameterization of U , Eq. (7).

If the neutrino mass spectrum is with IH, one has in this convention (see, e.g., [32, 36]):

$$\Delta m_{\odot}^2 = \Delta m_{32}^2 > 0, \quad \text{IH spectrum (B)}, \quad (18)$$

and

$$|U_{e2}| = \cos \theta_{\odot} \sqrt{1 - |U_{e1}|^2}, \quad |U_{e3}| = \sin \theta_{\odot} \sqrt{1 - |U_{e1}|^2}, \quad \text{IH spectrum (B)}. \quad (19)$$

The mixing matrix element of U constrained by the CHOOZ and Palo Verde data is now $|U_{e1}|^2$:

$$|U_{e1}|^2 = \sin^2 \theta, \quad \text{IH spectrum (B)}. \quad (20)$$

We would like to emphasize that Eqs. (9) and (10) are valid in the two conventions for the ordering of the neutrino masses discussed above.

Few comments are in order. The $\bar{\nu}_e$ survival probability depends only on the four continuous parameters Δm_{\odot}^2 , $\sin^2 \theta_{\odot}$, Δm_{atm}^2 , $\sin^2 \theta$, and on a single “discrete” parameter — the type of the neutrino mass spectrum — NH or IH. The terms in the second lines of Eq. (9) and Eq. (10) are responsible for the dominant effects in the survival probability for the intermediate baseline experiment under consideration in the case of the high-LMA solution of the solar neutrino problem. The study of the dominant oscillations can thus constrain the solar neutrino oscillation parameters. In a complete 3-neutrino oscillation analysis, one should also consider the effect of the terms in the first and third lines of Eq. (9) and Eq. (10). While the terms in the first lines give the sub-dominant, faster oscillations driven by Δm_{atm}^2 , the terms in the last lines are responsible for the difference between the probabilities corresponding to the NH and IH neutrino mass spectra. Both of them are suppressed by $\sin^2 \theta$. The detection of this sub-leading oscillatory behavior, controlled by the atmospheric neutrino mass squared difference, would be an indication of the non-vanishing of the mixing angle θ in the PMNS matrix U . It will also enable the experiment under discussion to determine Δm_{atm}^2 with a high precision. Finally, for sufficiently large values of $\sin^2 \theta$ it should in principle be possible to distinguish the normal from the inverted hierarchy spectrum. Let us stress that the difference of the survival probabilities for the NH and the IH spectra lies in the interference term: the existing solar neutrino and KamLAND data indicate that θ_{\odot} is not maximal, so that $\sin \theta_{\odot} \neq \cos \theta_{\odot}$. In ideal conditions in which Δm_{atm}^2 is known to a very high precision, $\sin^2 \theta$ is not too small, $\sin^2 2\theta_{\odot} \lesssim 0.90$, and the statistics and the energy resolution of the experimental

Power	Threshold	Baseline	Exposure	No osc
P (GW)	E_{th} (MeV)	L (km)	T (kTy)	Events
5	1.0	20	3	14971
5	2.6	20	3	10585
5	1.0	30	3	6654
5	2.6	30	3	4704
25	1.0	20	3	74855
25	1.0	30	3	33269

TABLE I: Number of events in the case of absence of $\bar{\nu}_e$ oscillations for the different reactor experimental set-ups considered in this paper.

apparatus are such to permit to resolve the Δm_{atm}^2 -driven oscillations, this could allow one to extract information about which of the two hierarchical neutrino mass patterns is realized in nature.

One can rewrite the term in parenthesis in the third line of Eq. (9) and Eq. (10) in the form:

$$\cos\left(\frac{\Delta m_{\text{atm}}^2 L}{2 E_\nu} - \frac{\Delta m_{\odot}^2 L}{2 E_\nu}\right) - \cos\frac{\Delta m_{\text{atm}}^2 L}{2 E_\nu} = 2 \sin\frac{\Delta m_{\odot}^2 L}{4 E_\nu} \sin\left(\frac{\Delta m_{\text{atm}}^2 L}{2 E_\nu} - \frac{\Delta m_{\odot}^2 L}{4 E_\nu}\right) \quad (21)$$

Thus, it consists of an oscillating function, with approximately the same frequency as the Δm_{atm}^2 -driven oscillations, modulated with period half of the usual Δm_{\odot}^2 -driven oscillations. In particular, the amplitude of this term is the maximal possible at values of L/E_ν where the survival probability goes to its Δm_{\odot}^2 -induced minima, and vanishes at its local maxima.

III. THE EXPERIMENT

Anti-neutrinos from nuclear reactor sources are detected through their inverse β -decay reaction with protons in the detector. The visible energy E_{vis} of the emitted positron is related to the energy of the incoming anti-neutrino E_ν and to the masses of the proton, neutron and positron as:

$$\begin{aligned} E_{\text{vis}} &\equiv E_\nu + m_{e^+} - (m_n - m_p), \\ &\simeq E_\nu - 0.8 \text{ MeV}. \end{aligned} \quad (22)$$

The E_{vis} spectrum of detected events in the no oscillation case, which takes into account the initial spectrum of anti-neutrinos emitted by the reactor and the inverse β -decay cross section, has a bell-shaped distribution, centered at about $E_{\text{vis}} \sim 2.8$ MeV. The total number of expected events for the no oscillation case is given in Table I. We consider a single reactor plant with power of either 5 GW (achievable, e.g., at Heilbronn, Germany [31]) or 25 GW (achievable at Kashiwazaki, Japan), as the only relevant source of neutrinos, neglecting the possible contaminations due to other plants at larger distances. We also assume that the reactors have a 100% efficiency. It is trivial to adapt our results to a given reactor efficiency. We present our results as function of the product of the exposure time and the active mass of the detector. We will assume for this product values in the range $3 \div 5$ kTy and consider baselines $20 \div 30$ km. The total statistics depends on $\mathcal{L} = P M T$, the product of the reactor power (P), the detector mass (M) and time of exposure (T), thus we express our results in units of GWkTy. Since the neutrino flux decreases as the inverse square of the baseline length, the shorter baselines obviously have much more statistics than the longer ones. We assume a liquid scintillation detector similar to ones used in the other reactor experiments like CHOOZ and KamLAND. We assume 8.48×10^{31} free protons per kton of detector mass as in KamLAND [6]. We use an energy resolution of $\sigma(E)/E = 5\%/\sqrt{E}$, E in MeV for “our” detector, assuming some improvement with respect to KamLAND, which reported a $\sigma(E)/E = 7.5\%/\sqrt{E}$ [6].

In Table I we present the number of no oscillation events for two different visible energy thresholds of 1.0 MeV and 2.6 MeV. While at higher energies the spectrum is known with relatively high accuracy, at lower energies a possible contamination from geophysical neutrinos and from the time variation of fuel composition is expected [37]. The KamLAND experiment puts a conservative lower threshold of $E_{\text{vis}} > 2.6$ MeV [6] to avoid the error associated with the geophysical neutrinos. However, since the reactor flux is the highest around 2.8 MeV, it is desirable to include

these parts of the energy spectrum to increase the statistical power of the experiment. We note from Table I that the number of observed events goes up by a factor of 1.4 when the effective threshold energy E_{th} is lowered from 2.6 MeV to 1.0 MeV. Further, with a larger energy window to be used in the data analysis, and correspondingly a large interval in L/E_ν , it is possible, in principle, to reconstruct a larger number of Δm_{atm}^2 -driven oscillation periods, and even to detect both the SPMIN and SPMAX connected to the Δm_{\odot}^2 -driven oscillations. The latter is crucial for the study of sub-leading effects performed in the second part of this paper.

The ratio of the number of events expected from geophysics sources to the total number of antineutrinos detected can be estimated for a given experimental set-up. In their first published data [6], KamLAND estimated the number of these spurious events to be 9, while the total data set contained 32 events with energy below the energy cut-off ($E_{th} = 2.6$ MeV) and 54 above this threshold. For KamLAND this ratio therefore comes up to be about 30% below 2.6 MeV. However, the number of background events due to the geophysical neutrinos is quite model dependent and a very good understanding and modeling (see, e.g., [38]) of the energy spectrum of these events would allow one to use the whole data sample in the range (1.0 – 7.2) MeV, by subtracting the geophysics background from the observed event spectrum, with just an additional source of systematics in the analysis – the extent of the uncertainty depending on the accuracy of the knowledge of the geophysical neutrino background.

The whole e^+ -energy spectrum could also be used in a very high statistics experiment with a sufficiently powerful reactor source. The contamination of the data sample from geophysical neutrino background at low energies is proportional to the active mass of the detector. Thus, decrease in the detector volume compensated with an increase in the reactor antineutrino flux, results in a reduction of the fraction of events due to this background. We can determine the flux of $\bar{\nu}_e$ from a reactor in the absence of oscillations as a function of the distance traveled and of the power of the source:

$$\Phi \equiv \frac{P}{L^2}. \quad (23)$$

For KamLAND, summing over all the reactors which contribute (see for instance [39] for a complete listing), one gets

$$\Phi^{\text{Kam}} \simeq 3 \times 10^{-3} \text{ GW/km}^2. \quad (24)$$

As a comparison, using three possible choices for the pair ($L/\text{km}, P/\text{GW}$) as (30, 5), (20, 5) and (20, 24), one gets for Φ values that are bigger by a factor of 1.5, 4 and 20, respectively. Accordingly, the fraction of background events from the geophysical neutrinos can be reduced by this factor, as a consequence of the larger flux. In particular, for the last case, the geophysical neutrinos contribution would be at the percent level even for a 1 kiloton detector like KamLAND and could be safely accounted for. For lower fluxes and large detectors, either a very accurate subtraction procedure needs to be applied, or it would be necessary to keep the cutoff in the low energy part of the spectrum as in KamLAND. In this paper we neglect throughout the contribution coming from geophysical neutrinos – we either put an energy threshold of 2.6 MeV, or when we lower E_{th} to 1.0 MeV we assume that either they can be accounted for, or they can be safely neglected.

Backgrounds may also result from radioactive impurities and from cosmic ray interactions. However, these can be effectively suppressed in realistic experiments [31] and we completely neglect backgrounds in this paper.

In presence of neutrino oscillation, the detected energy spectrum at a distance L from the reactor is obtained by convoluting the survival probability given by Eq. (9) or Eq. (10) with the spectrum obtained with no oscillation. This leads to a suppression of the number of detected events, and to a distortion of the energy spectrum itself, whose dependence on the parameters entering the survival probabilities may be used to extract them through a χ^2 fit of the data.

The optimal distance in order to resolve the first minimum (SPMIN) of the survival probability, and extract with good accuracy a measurement of Δm_{\odot}^2 and $\sin^2 \theta_{\odot}$, according to Eq. (9) and Eq. (10), is given by ⁶ :

$$L^* \equiv \frac{2\pi E_\nu}{\Delta m_{\odot}^2}, \quad (25)$$

so that its choice depends on the actual value of Δm_{\odot}^2 and on the typical energy involved. If E_ν is at the peak of the spectrum (3.5 ÷ 4 MeV), this choice implies a maximal depletion of the total number of events. We will consider always the case in which a relatively large statistics is accumulated, so that the main source of information is the differential

⁶ This distance is also the optimal one for enhancing the effect of the interference term in the survival probability distinguishing the NH and IH spectrum cases, as seen from Eq. (21), because for this values of L/E_ν the modulation of the beating-like term is maximal.

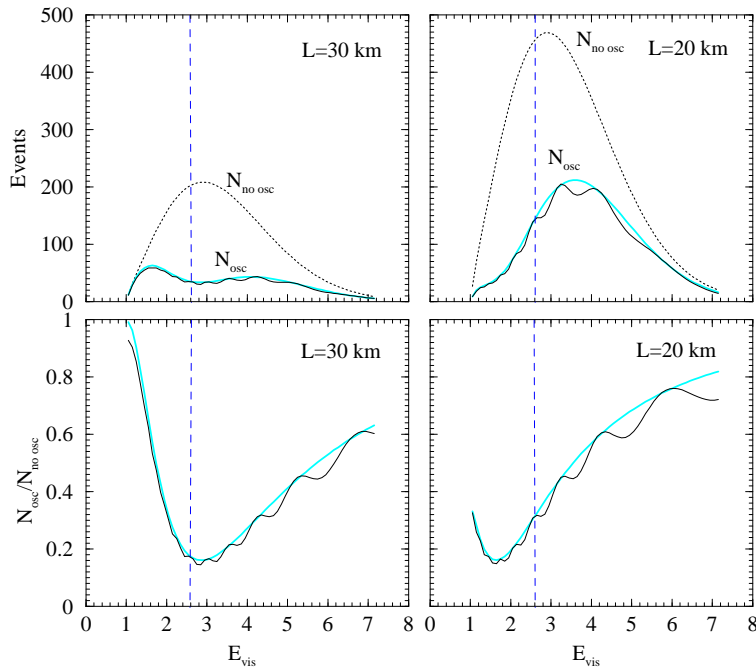


FIG. 2: The observed e^+ –energy spectrum (in 0.1 MeV bins) for the 20 km (right-panel) and 30 km (left-panel) experiment with reactor power 5 GW and exposure of 3 kTy (15 GWkTy). The dotted black lines in the top panels give the number of events in the absence of oscillations. The solid lines give the events for $\bar{\nu}_e$ –oscillations with $\Delta m_{\odot}^2 = 1.5 \times 10^{-4} \text{ eV}^2$, $\sin^2 \theta_{\odot} = 0.3$, $\Delta m_{\text{atm}}^2 = 2.5 \times 10^{-3} \text{ eV}^2$. The solid cyan/grey line corresponds to the spectrum for $\sin^2 \theta = 0.0$, while the solid black line shows the spectrum for $\sin^2 \theta = 0.03$. The bottom panels show the corresponding ratio of events in the cases of $\bar{\nu}_e$ –oscillations and of absence of oscillations for the two values of $\sin^2 \theta$. The event spectra in the case of $\bar{\nu}_e$ –oscillations are for neutrino mass spectrum with normal hierarchy.

energy spectrum of detected events. In this case a large window of different energies can be used to determine L^* . However, as long as the baseline of the experiment is large enough to include the first oscillation minimum (SPMIN) in the interval of energies used for the measurements, preferably in the part of the energy spectrum with highest statistics, the experiment is expected to display a good sensitivity to the solar neutrino oscillation parameters.

We show in Fig. 2 the spectrum of observed events for two specific baselines of 20 km and 30 km for reactor power of 5 GW and 3 kTy exposure. We note that the 30 km experiment has much less events than the 20 km experiment. The solid lines in the bottom panels show that the SPMIN for the 30 km experiment comes around 2.8 MeV, where the flux is the highest. For the 20 km experiment the SPMIN comes at around 1.6 MeV. Correspondingly, if the lower energy cut-off is set to $E_{th} = 2.6 \text{ MeV}$ (shown by the dashed lines in Fig. 2), the 20 km experiment would miss the SPMIN. Therefore for the 20 km experiment, the E_{th} has to be lowered to below 1.6 MeV if the value of Δm_{\odot}^2 happens to be $1.5 \times 10^{-4} \text{ eV}^2$. For higher values of Δm_{\odot}^2 , the SPMIN will shift to higher energies and the threshold could be taken higher: for $\Delta m_{\odot}^2 = 2.5 \times 10^{-4} \text{ eV}^2$, for instance, SPMIN is at $E_{vis} = 3.2$ (5.3) MeV for $L = 20$ (30) km.

Figure 2 also shows the “sub-dominant” oscillation effects dependent on Δm_{atm}^2 and $\sin^2 \theta$, imprinted on the large dominant oscillation wave driven by the solar neutrino oscillation parameters. The experiment could be expected to have sensitivity to the parameters Δm_{atm}^2 and $\sin^2 \theta$, driving the sub-dominant oscillations, if the energy resolution of the detector would be good enough to enable a large statistics experiment like the one we consider here, to break the total number of events into fine energy bins. In particular, to resolve the oscillatory behavior one needs bins much smaller than the oscillation period

$$\Delta E \ll \Delta E^* \equiv \frac{4\pi E_{\nu}^2}{\Delta m^2 L}, \quad (26)$$

where Δm^2 is the relevant neutrino mass squared difference driving the oscillations. This implies that for a given L , higher energy resolution and smaller bins are required in order to resolve effects due to a larger mass squared difference. As a numerical example,

$$\Delta m_{\odot}^2 = 1.5 \times 10^{-4} \text{ eV}^2 \implies \Delta E_{\odot}^* = 7.1 \text{ MeV},$$

$$\Delta m_{\text{atm}}^2 = 2.7 \times 10^{-3} \text{ eV}^2 \implies \Delta E_{\text{atm}}^* = 0.4 \text{ MeV},$$

for energies at the peak of the spectrum ($E_\nu = 3.6 \text{ MeV}$) and at the distance $L = 30 \text{ km}$. It is clear that energy bins with a width of 0.425 MeV (as in KamLAND) allow a good reconstruction of the spectral distortion due to Δm_{\odot}^2 -driven oscillations, but would average out completely the sub-leading Δm_{atm}^2 effects. Using as a guide rule the assumption that to resolve an oscillation one needs $\Delta E_{\text{vis}} \lesssim \Delta E^*/4$, the reconstruction of Δm_{atm}^2 -driven oscillations requires to use energy bins having width of $\sim 0.1 \text{ MeV}$. The use of shorter distances can soften this problem, as Eq. (26) indicates. However, with an energy resolution of $\sigma(E)/E = 5\%/\sqrt{E}$, it should be possible to have bins of size of 0.1 MeV , at least as long as the energy is not very large. We will show that with bins of 0.1 MeV width, and $L = 20 \text{ km}$, one can improve on the CHOOZ limit for $\sin^2 \theta$, and if $\sin^2 \theta$ is found to be large enough to be detectable in this experiment, Δm_{atm}^2 can be determined with a very high precision.

With an experimental set-up which allows a sufficiently small bin size and large enough statistics to measure the sub-dominant oscillations, one can hope to gain information about the neutrino mass hierarchy using the last interference terms in Eq. (9) and Eq. (10).

Finally, one has to take into account the presence of systematic errors both in the determination of the flux normalization and in the energy calibration of the detector. The KamLAND collaboration estimated a total systematic uncertainty of about 6.42% in their first published analysis [6]. The bulk of this error comes from uncertainty in the overall flux normalization. The use of a near detector can improve this flux normalization error to as low as 0.8% [31]. The error on energy calibration could be taken as 0.5% [41]. We use a total systematic uncertainty of 2%, and we discuss in detail the effect of varying this uncertainty in the analysis which follows.

IV. PRECISION NEUTRINO OSCILLATION PHYSICS : Δm_{\odot}^2 AND $\sin^2 2\theta_{\odot}$ IN THE HIGH-LMA REGION

In this Section we study quantitatively the precision measurements of the solar neutrino oscillation parameters Δm_{\odot}^2 and $\sin^2 \theta_{\odot}$, possible in the intermediate baseline reactor experiment discussed in the previous section under the assumption that Δm_{\odot}^2 lies in the high-LMA region. We simulate the “data” at certain plausible values of Δm_{\odot}^2 and $\sin^2 \theta_{\odot}$ and obtain allowed regions in the parameter space from a dedicated χ^2 analysis. For the errors we assume a Gaussian distribution and define our χ^2 as

$$\chi^2 = \sum_{i,j} (N_i^{\text{data}} - N_i^{\text{theory}})(\sigma_{ij}^2)^{-1}(N_j^{\text{data}} - N_j^{\text{theory}}), \quad (27)$$

where N_i^α ($\alpha = \text{data}, \text{theory}$) is the number of events in the i^{th} bin, σ_{ij}^2 is the covariant error matrix containing the statistical and systematic errors and the sum is over all bins. We compare the sensitivities obtained for two possible baselines, 20 km and 30 km. To quantify the sensitivity we define the relative precision p_a for a certain parameter a at a given C.L. as

$$p_a = \frac{a_{\text{max}} - a_{\text{min}}}{a_{\text{max}} + a_{\text{min}}}, \quad (28)$$

where a_{max} (a_{min}) are the maximal (minimal) allowed value of a found at the chosen C.L. We check quantitatively the impact of (1) the energy threshold E_{th} , (2) bin size ΔE and (3) systematic uncertainties. We also show the impact of increasing the statistics by a factor of 5.

As has been noted earlier in the context of KamLAND [40], the sensitivity to $\sin^2 \theta_{\odot}$ can be reduced considerably by the uncertainty in the parameter $\sin^2 \theta$. We therefore analyze first the impact this uncertainty can have on the precision of $\sin^2 \theta_{\odot}$ determination in the intermediate baseline reactor experiment of interest. Since the baseline is optimized to measure predominantly the Δm_{\odot}^2 -driven oscillations, we assume that the Δm_{atm}^2 -driven oscillations are averaged out. This corresponds to the realistic case of using a sufficiently large e^+ -energy bin size. The expression for the survival probability would then reduce to

$$P_{ee} \approx \cos^4 \theta \left(1 - \sin^2 2\theta_{\odot} \sin^2 \frac{\Delta m_{\odot}^2 L}{4 E_\nu} \right), \quad (29)$$

where we have neglected the term $\sim \sin^4 \theta$. Therefore the uncertainty in $\sin^2 \theta$ essentially brings up to a $\sim 10\%$ uncertainty in the $\bar{\nu}_e$ survival probability. Since the factor $\cos^4 \theta$ can only reduce the survival probability, it does not affect the upper limit on the allowed range of $\sin^2 \theta_{\odot}$. However, it can have an effect on the lower limit on

$\sin^2 \theta_\odot$ reducing it further, and thus can worsen, in principle, the precision of the experiment. Using eq. (29) we get approximately for the *additional* error on $\sin^2 2\theta_\odot$ due to the uncertainty in the value of $\sin^2 \theta$

$$\delta(\sin^2 2\theta_\odot) \approx \frac{2\Delta P_{ee} \sin^2 \theta}{\sin^2 \frac{\Delta m_\odot^2 L}{4E_\nu}} + 2 \frac{(1 - \sin^2 2\theta_\odot \sin^2 \frac{\Delta m_\odot^2 L}{4E_\nu}) \Delta(\sin^2 \theta)}{\sin^2 \frac{\Delta m_\odot^2 L}{4E_\nu}}, \quad (30)$$

where ΔP_{ee} and $\Delta(\sin^2 \theta)$ are the uncertainties in the determination of the survival probability and $\sin^2 \theta$, respectively. We work in a scenario in which one would use the SPMIN in order to determine $\sin^2 2\theta_\odot$. In the SPMIN region one has $\sin^2(\Delta m_\odot^2 L/4E_\nu) \sim 1$ and therefore

$$\delta(\sin^2 2\theta_\odot) \approx 2\Delta P_{ee} \sin^2 \theta + 2 \cos^2 2\theta_\odot \Delta(\sin^2 \theta). \quad (31)$$

Thus, in this SPMIN scenario, the first term gives an extra contribution of about $2\Delta P_{ee} \sin^2 \theta$ to the allowed range of $\sin^2 2\theta_\odot$. Since, as we will see in the present Section, in the experiment under consideration the allowed range of $\Delta P_{ee} \lesssim 0.1$ even under the most conservative conditions, this term gives an extra contribution to the allowed range which is $\lesssim 0.01$. The second term is independent of the precision of a given experiment (i.e., on ΔP_{ee}) and depends only on the best-fit value of $\cos^2 2\theta_\odot$ and on the error in $\sin^2 \theta$. For the current 3σ error in $\sin^2 \theta$ of 0.05 and best-fit $\cos^2 2\theta_\odot$ of 0.16, this would give an increase of only 0.018. The suppression of this term is mainly due to the presence of the factor $\cos^2 2\theta_\odot$ which is a relatively small number for the current best-fit solution. Thus, even though the uncertainty in $\sin^2 \theta$ brings a 10% uncertainty in the value of P_{ee} , it increases the allowed range of $\sin^2 2\theta_\odot$ only by $\lesssim (2 - 3)\%$, if one uses the SPMIN region for the $\sin^2 2\theta_\odot$ determination.

The error in the measured value of $\sin^2 2\theta_\odot$ due to the uncertainty in the value of $\sin^2 \theta$ is considerably larger in an experiment like KamLAND, which is sensitive primarily to the region of the maximum of the $\bar{\nu}_e$ survival probability⁷ (SPMAX). In this case the oscillatory term $\sin^2(\Delta m_\odot^2 L/4E_\nu) \neq 1$ and can be quite small, so that the extra contribution to the uncertainty in $\sin^2 2\theta_\odot$, given roughly by Eq. (30), would be rather large. The first term in the expression in the right-hand side of Eq. (30) becomes relatively large due to presence of the oscillatory term in the denominator and the second term becomes even larger due to the presence of the same term both in the denominator and in the numerator. Thus, for KamLAND the impact of the uncertainty in $\sin^2 \theta$ on $\sin^2 \theta_\odot$ determination is essentially related to the fact that the Δm_\odot^2 -dependent oscillatory term for KamLAND is relatively small, resulting in rather big contributions from both terms in Eq. (30). This explains the relatively large effect of the $\sin^2 \theta$ uncertainty on the $\sin^2 2\theta_\odot$ determination noticed in [40]. We assert that to reduce the impact of the $\sin^2 \theta$ uncertainty on the determination of $\sin^2 \theta_\odot$, one needs to “tune” the experiment to the SPMIN. This observation gives further credence to our statement that the best experimental set-up for determining the solar neutrino mixing angle with high precision is a reactor experiment sensitive to the SPMIN.

In Figs. 3 and 4 we show the regions of allowed values of Δm_\odot^2 and $\sin^2 \theta_\odot$, obtained with “data” simulated at various values of $\Delta m_\odot^2 > 1.0 \times 10^{-4} \text{ eV}^2$ and $\sin^2 \theta_\odot = 0.3$. We assume a statistics corresponding to an exposure of 15 GWkTy (5GW \times 3kTy) [31], bin size $\Delta E = 0.425 \text{ MeV}$ and plausible systematic uncertainty of 2%. Figure 3 shows the allowed regions obtained for $\sin^2 \theta = 0$, corresponding to the case of 2-neutrino Δm_\odot^2 -driven oscillations. In Fig. 4 we display the corresponding allowed regions in a complete 3-neutrino mixing scheme with $\sin^2 \theta$ allowed to vary freely within the 99.73% C.L. allowed range, $\sin^2 \theta < 0.05$. As a comparison of the two figures indicates, the effect of keeping $\sin^2 \theta$ free, on the allowed ranges of the solar neutrino oscillation parameters in general, and on $\sin^2 \theta_\odot$ in particular, is rather small. This is compatible with the conclusions of the analysis presented above. To further substantiate our point pertaining to the impact of the $\sin^2 \theta$ uncertainty, we show in Fig. 5 a blow-up of the 99.73% C.L. contours for the $\sin^2 \theta$ free (within the bound $\sin^2 \theta < 0.05$) and the $\sin^2 \theta = 0$ cases, obtained with $L = 30 \text{ km}$, $E_{th} = 2.6 \text{ MeV}$ and with assumed “true” value of $\Delta m_\odot^2 = 1.5 \times 10^{-4} \text{ eV}^2$. We stress that the effect of keeping $\sin^2 \theta$ free is small and henceforth in the rest of this Section neglect the effect of $\sin^2 \theta$ uncertainty on the precision of the Δm_\odot^2 and $\sin^2 \theta_\odot$ determination.

In Fig. 3 we compare the precision obtained on the solar neutrino oscillation parameters for two intermediate baselines of 20 km and 30 km, with and without imposing the low energy cut-off of 2.6 MeV⁸. For the baseline of $L = 30 \text{ km}$, depending on the “true” values of the parameters, at 99% C.L. a precision respectively of (6 – 7)% and (3 – 6)% is possible to achieve for $\sin^2 \theta_\odot$ and Δm_\odot^2 even with $E_{th} = 2.6 \text{ MeV}$. These errors reduce only slightly

⁷ This is valid both for $\Delta m_\odot^2 \sim 7.2 \times 10^{-5} \text{ eV}^2$ and for $\Delta m_\odot^2 \sim 1.5 \times 10^{-4} \text{ eV}^2$.

⁸ For all the cases we get two solutions in $\sin^2 \theta_\odot$, the real one and a “fake” one on the “dark-side” ($\sin^2 \theta_\odot > 0.5$). This fake “dark-side” solutions are ruled out by the solar neutrino data. Nonetheless we show them in our plots for the sake of completeness.

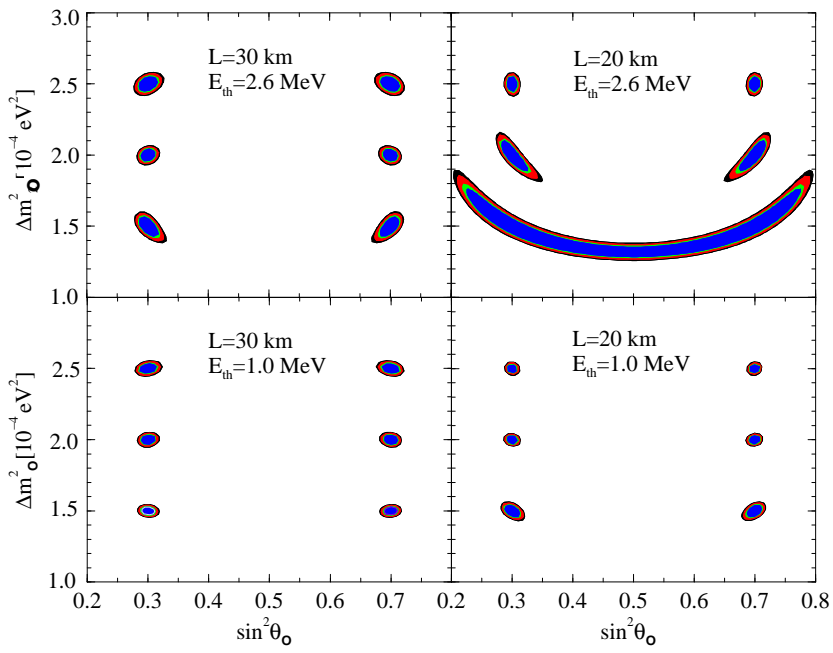


FIG. 3: Simulated two parameter fit of the e^+ –energy spectrum in the $\Delta m_{\odot}^2 - \sin^2 \theta_{\odot}$ plane. We assume $\sin^2 \theta = 0$, $\sin^2 \theta_{\odot} = 0.3$ and vary the value of Δm_{\odot}^2 . We compare results at $L = 20$ km and $L = 30$ km, with the lower cut-off on the energy spectrum at $E_{th} = 2.6$ MeV and at $E_{th} = 1.0$ MeV. The energy bin size is chosen as $\Delta E = 0.425$ MeV, systematic uncertainties are taken as 2% and the statistics correspond to 15 GWkTy. Shown are the 90%, 95%, 99% and 99.73% (3σ) C.L. contours.

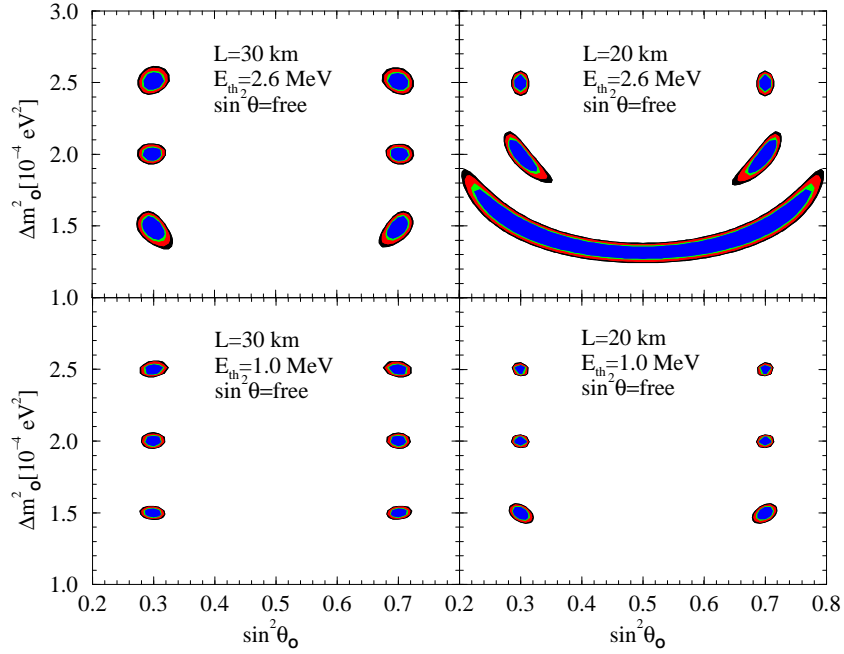


FIG. 4: The same as in Fig. 3 but for $\sin^2 \theta$ allowed to vary freely within its 99.73% C.L. allowed range, $\sin^2 \theta < 0.05$.

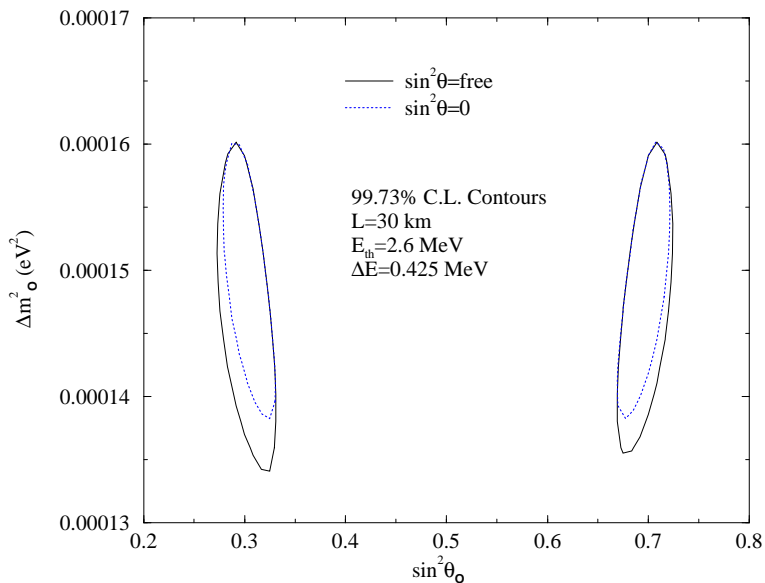


FIG. 5: Comparison of the allowed regions obtained at the 99.73% C.L. for $\sin^2 \theta = 0$ and allowing $\sin^2 \theta$ to vary freely within its 99.73% C.L. allowed range, $\sin^2 \theta < 0.05$. The curves correspond to the top left-hand panels of Figs. 3 and 4 and “true” $\Delta m_{\odot}^2 = 1.5 \times 10^{-4} \text{ eV}^2$.

to (5–6)% and $\sim 2\%$, respectively, when the threshold is lowered to 1.0 MeV, owing mainly to the fact that the statistics increases, but also to the fact that the SPMIN is fully used in the measurement.

For the $L = 20 \text{ km}$ experiment on the other hand, the precision for both Δm_{\odot}^2 and $\sin^2 \theta_{\odot}$ (and especially for $\sin^2 \theta_{\odot}$) is relatively low if the effective threshold of $E_{th} = 2.6 \text{ MeV}$ is applied, and if $\Delta m_{\odot}^2 = 1.5 \times 10^{-4} \text{ eV}^2$. As discussed in the previous Section, for larger values of Δm_{\odot}^2 which produce the SPMIN at $E_{vis} > 2.6 \text{ MeV}$, it is still possible to reach high precision in the determination of $\sin^2 \theta_{\odot}$ and Δm_{\odot}^2 even with the cut-off of $E_{th} = 2.6 \text{ MeV}$. These values are somewhat disfavored by the current data [11, 12, 13]. If the threshold is lowered to 1.0 MeV, the experiment can “see” the full SPMIN even for $\Delta m_{\odot}^2 = 1.5 \times 10^{-4} \text{ eV}^2$ and the sensitivity to both Δm_{\odot}^2 and $\sin^2 \theta_{\odot}$ becomes remarkable. The Δm_{\odot}^2 can be determined with a $\sim 2\%$ precision, while the $\sin^2 \theta_{\odot}$ would be known to within $\sim (3-4)\%$, at the 99% C.L. With $E_{th} = 1.0 \text{ MeV}$ even though both $L = 20 \text{ km}$ and $L = 30 \text{ km}$ baseline experiments would be sensitive to SPMIN, the precision of the shorter baseline experiment is higher, owing to the larger statistics expected.

In Fig. 6, we study the effect of using smaller bins in the e^+ –energy spectrum. As explained in the previous Section, there is no substantial improvement in the precision of the fit to the solar neutrino oscillation parameters Δm_{\odot}^2 and $\sin^2 \theta_{\odot}$ with this strategy. The binning energy used by KamLAND ($\Delta E = 0.425 \text{ MeV}$) is already sufficient and one does not need to use smaller bins. However, we will see in the next sections that a better energy resolution could allow for the extraction of other information embedded in the sub-dominant oscillations.

One of the crucial issues in these types of experiments is thought to be the control of the systematic error. Indeed, a large systematic uncertainty on the energy spectrum could threaten to wash out the possibility of extracting any information from the data. In Fig. 7 we show the impact of the systematic uncertainty on the expected precision. The plots show the allowed areas obtained assuming 1% and 3% systematic uncertainties and can be compared with the lower panels in Fig. 3, where the systematic uncertainty is taken as 2%. By comparing the relative precision on the parameters, we note that while the precision on Δm_{\odot}^2 remains essentially unaffected by the exact value of the systematic uncertainty if the latter does not exceed $\sim 4\%$, the precision of $\sin^2 \theta_{\odot}$ may show a very mild dependence, the error in $\sin^2 \theta_{\odot}$ obviously decreasing with the reduction in the systematic error. However, the impact is not large (see also [29] where the performance of KamLAND is studied under assumption of various anticipated systematic errors). This implies that, at least for reasonably small values of the systematic uncertainties, their impact on the precision of the parameter determination is only marginal. This result is essentially due to the fact that we are assuming rather large statistics, allowing for a good reconstruction of the oscillatory pattern in the energy spectrum. Similar conclusions were recently drawn in the context of a short baseline experiment at nuclear reactors ($L = 1.7 \text{ km}$) in [41].

By contrast, we illustrate in Fig. 8 the huge effect that an increase in the statistical sample could lead to. We show

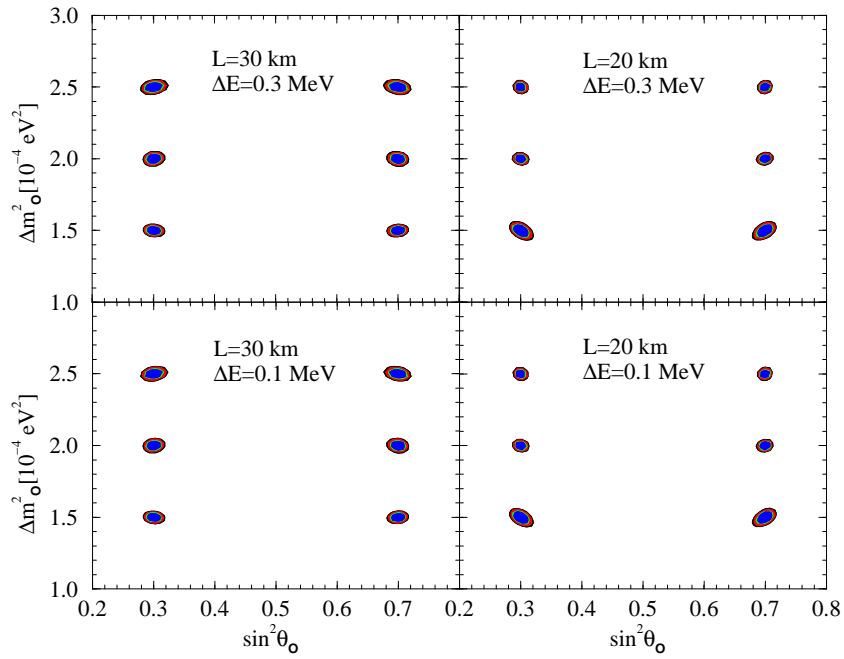


FIG. 6: The same as the lower panels in Fig. 3, but showing the effect of reducing the e^+ -energy bin size ΔE .

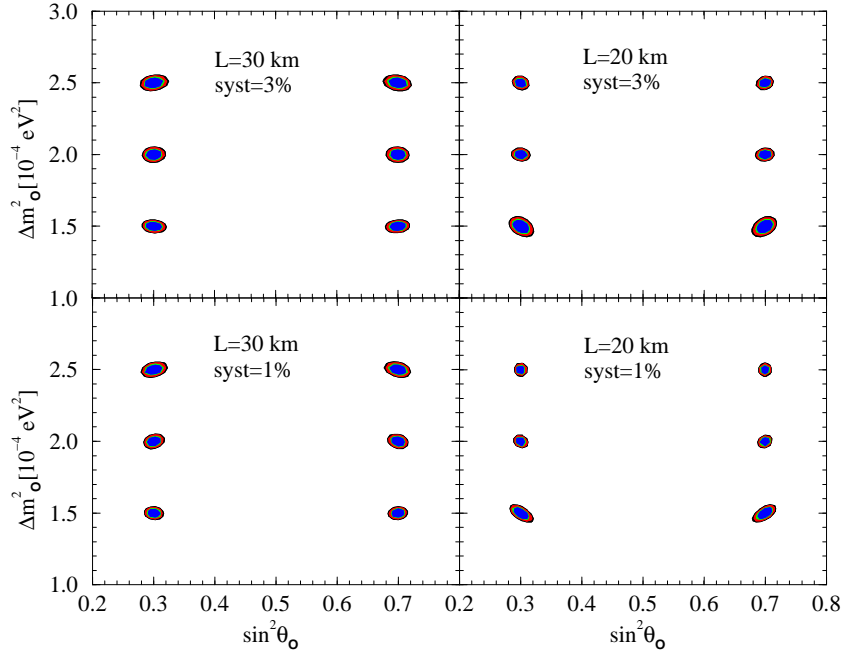


FIG. 7: The same as the lower panels in Fig. 3 but showing the effect of varying the systematic error.

the allowed regions, corresponding to Fig. 3, that would be obtained if the statistics were increased 5 fold. This could be done using a reactor complex of total power comparable to the Kashiwazaki site (24.3 GW) and a large enough detector. We note that the error in the statistical determination of both Δm_{\odot}^2 and $\sin^2 \theta_{\odot}$ would go down below the percent level. With this statistics even the effect of the systematic uncertainty on the precision determination of the parameters is expected to be low and one can achieve remarkable accuracy.

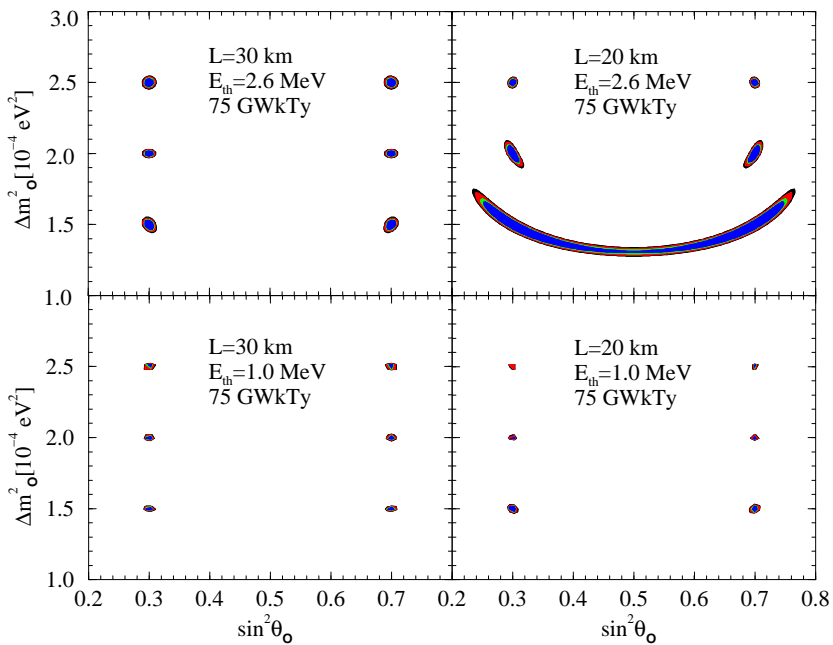


FIG. 8: The same as in Fig. 3, but showing the effect of increasing the statistics five times, corresponding to 75 GWkTy.

V. PRECISION PHYSICS FROM Δm_{atm}^2 -DRIVEN (SUB-DOMINANT) OSCILLATIONS

In this Section we will consider the set-up where the experiment could be sensitive to the Δm_{atm}^2 -driven sub-dominant oscillations. As discussed in Section III, one has to use relatively small energy bins in order to observe these oscillation effects. We first consider the potential of the intermediate baseline reactor experiment of interest in improving the bound on $\sin^2 \theta$. We next assume that $\sin^2 \theta$ is sufficiently large and can therefore lead to observable Δm_{atm}^2 -driven oscillations and investigate under what conditions one can use these “fast” oscillations to determine Δm_{atm}^2 with a high precision. Finally, we study the possibility of achieving what is probably a most ambitious goal – to get information on the neutrino mass hierarchy by observing the reactor $\bar{\nu}_e$ oscillations at intermediate baselines.

A. Improving the Limit on $\sin^2 \theta$

We investigate in what follows the impact of several experimental conditions on the achievable sensitivity on $\sin^2 \theta$. We show in Fig. 9 the $\sin^2 \theta$ sensitivity obtainable in a 15 GWkTy statistics experiment. We generate the “data” at $\sin^2 \theta = 0$ and at each value of $\sin^2 \theta$ we plot the difference between the χ^2 function obtained at that value of $\sin^2 \theta$ and the χ_{min}^2 , which obviously comes at $\sin^2 \theta = 0$. We define the 3σ and 90% C.L. limit levels as $\Delta\chi^2 = 9$ and 2.71, respectively, corresponding to a one parameter fit.

The sensitivity to $\sin^2 \theta$ increases substantially if the baseline L is reduced. It follows from Eq. (25) that the best sensitivity to $\sin^2 \theta$ is achieved for $L = \text{few km}$ [41, 42]. The intermediate baselines we are considering are not optimized for the measurement of θ . The sensitivity to $\sin^2 \theta$ of the experiment under discussion is worse than that of the experiment proposed recently in [41, 42] with a distance of 1.7 km. Still, the experiment with $L = 20$ km, would allow to put an upper bound of

$$\sin^2 \theta < 0.021 \text{ (0.012)}, \quad (32)$$

at the 3σ (90%) C.L. (Fig. 9, top left panel), which is a noticeable improvement over the current 3σ bound of $\sin^2 \theta < 0.05$.

Rather relevant for the sensitivity to $\sin^2 \theta$, in addition to the distance L , is the width of the final state e^+ energy bins. As could be expected, the smaller bins give a better sensitivity to the value of $\sin^2 \theta$. Bins with width of 0.1 MeV give a 50% improvement in sensitivity compared to the case of bin width of 0.425 MeV. Another relevant factor is the presence of a low energy cut-off in the part of the spectrum used in the fit: the sensitivity improves with the

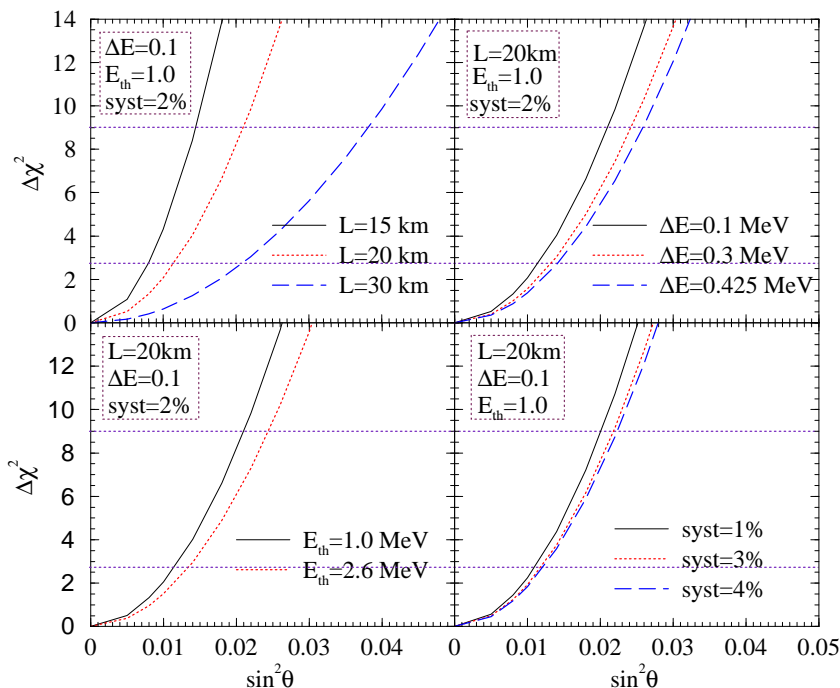


FIG. 9: Study of the sensitivity to $\sin^2 \theta$. Shown are the $\Delta\chi^2$ obtained as a function of $\sin^2 \theta$, when fitting a simulated “data” set generated for $\sin^2 \theta = 0$, $\Delta m_{\text{atm}}^2 = 2.5 \times 10^{-3} \text{ eV}^2$, $\Delta m_{\text{atm}}^2 = 1.5 \times 10^{-4} \text{ eV}^2$ and $\sin^2 \theta_{\odot} = 0.3$. For a particular value of $\sin^2 \theta$, the other parameters are allowed to vary freely in the fit. The two horizontal lines correspond to 3σ and 90% C.L., respectively. We assume a total exposure of $\mathcal{L} = 15 \text{ GWkTy}$, and explore the impact of the baseline (L), width of energy bins (ΔE), the systematic uncertainties and the application of a low-energy cut-off (E_{th}) on the $\sin^2 \theta$ sensitivity.

inclusion of the lower energy data by, e.g., changing the cut-off energy from 2.6 MeV to 1.0 MeV. Finally, the last panel in Fig. 9 illustrates the effect of the systematic uncertainties on the sensitivity to $\sin^2 \theta$. As discussed in detail in the previous Section, the systematic error in the $\sin^2 \theta$ measurement has a small but non-negligible effect – the limit improving marginally with the reduction of the error.

We show in Fig. 10 the $\sin^2 \theta$ sensitivity when the statistics are increased by a factor of five: we consider statistics corresponding to 75 GWkTy. Clearly, the increase in statistics improves the $\sin^2 \theta$ sensitivity and at 3σ (90% C.L.) limit for the $L = 20$ baseline case reads (Fig. 10, top left panel)

$$\sin^2 \theta < 0.01 \text{ (0.0055)}. \quad (33)$$

Thus, for these very high statistics we get a sensitivity to $\sin^2 \theta$ which is almost of the same order as that expected to be reached in the “Reactor-I” experiment discussed in [41]. Note that with the increase of the statistics, the effect of both the systematic error and of the value of E_{th} chosen on the $\sin^2 \theta$ sensitivity decreases. The decreasing of the energy bin size, however, has essentially the same effect of increasing the sensitivity.

B. Measuring Δm_{atm}^2 and $\sin^2 \theta$

The experimental setup we consider is optimized for extremely precise measurement of θ_{\odot} , Δm_{\odot}^2 , and for distinguishing which hierarchy is realized in the neutrino mass spectrum (as we will see in the next Section), provided the high-LMA solution is the correct one. Nevertheless, in order to achieve these goals, a relatively large statistics and a sufficiently good energy resolution are required. With these favorable conditions fulfilled and bin width of 0.1 MeV, one could hope to improve on the precision of Δm_{atm}^2 and $\sin^2 \theta$, provided $\sin^2 \theta$ is non-zero and is sufficiently large. *We will show that both of these measurements are rather independent of the value of Δm_{\odot}^2 , so that they could be performed in this type of an experiment even if the low-LMA solution is confirmed by the KamLAND collaboration.*

In Fig. 11 we show the allowed regions in the $\Delta m_{\text{atm}}^2 - \sin^2 \theta$ plane, obtained for $L = 20 \text{ km}$ and two different statistics samples: the top panels correspond to 15 GWkTy, while the lower panels are for a 75 GWkTy exposure.

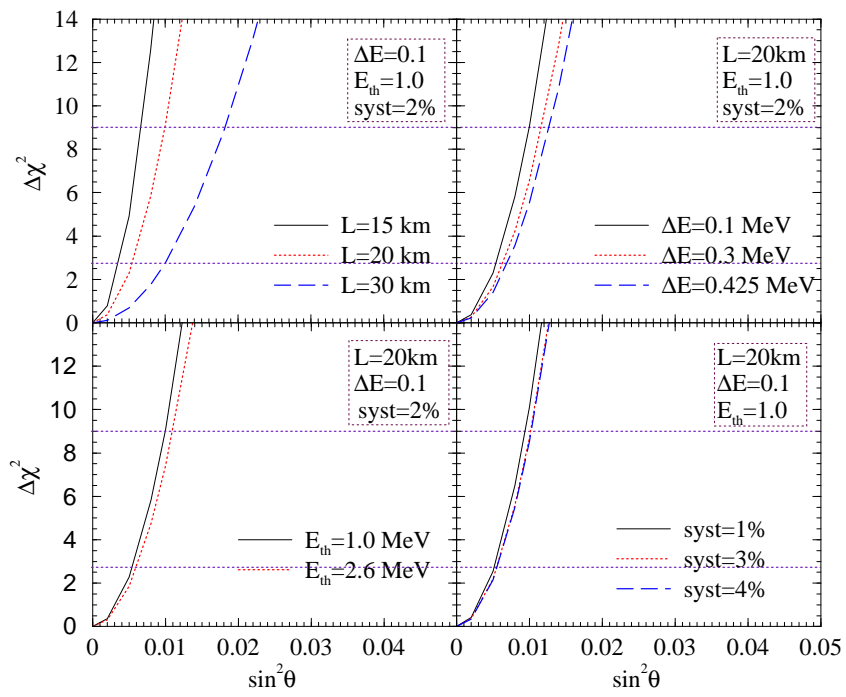


FIG. 10: The same as in Fig. 9, but with statistics increased by a factor of five ($\mathcal{L} = 75$ GWkTy).

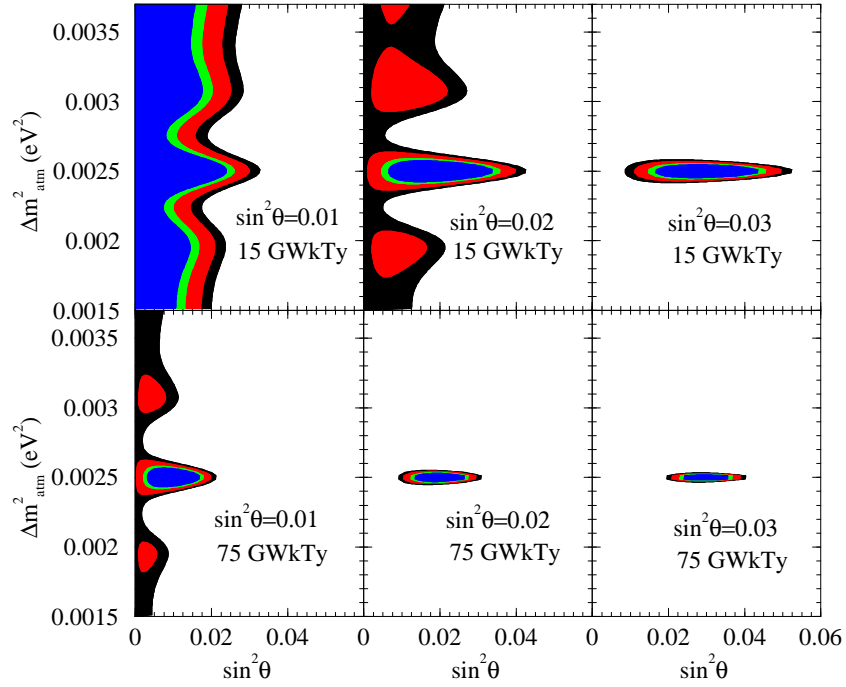


FIG. 11: The 90%, 95%, 99% and 99.73% C.L. allowed regions obtained by fitting “data” set simulated at $\Delta m_{\text{atm}}^2 = 2.5 \times 10^{-3}$ eV² and three different “true” values of $\sin^2 \theta$. The solar parameters Δm_{\odot}^2 and $\sin^2 \theta_{\odot}$ are taken to be 1.5×10^{-4} eV² and 0.3, respectively. The statistics assumed corresponds to $\mathcal{L} = 15$ GWkTy for the upper panels and to $\mathcal{L} = 75$ GWkTy for the lower panels. The distance used is $L = 20$ km. The bin size is taken as 0.1 MeV, the lower energy cut-off is $E_{th} = 1.0$ MeV, and the systematic uncertainty is assumed to be 2%. Both the “data” set and the fitted e^+ -spectrum correspond to NH neutrino mass spectrum.

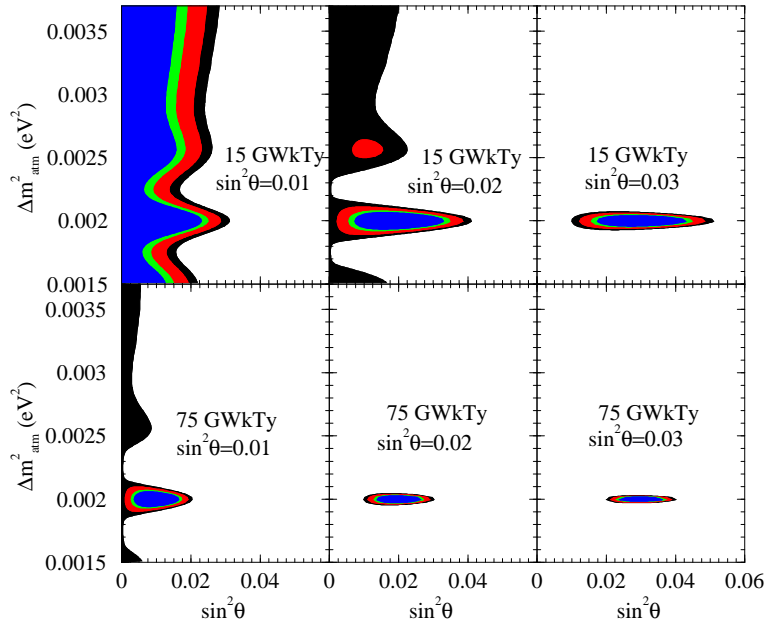


FIG. 12: The same as in Fig. 11, but assuming that the “true” value of $\Delta m_{\text{atm}}^2 = 2 \times 10^{-3} \text{ eV}^2$.

The results shown in Fig. 11 are for three different “true” values of $\sin^2 \theta$ and for $\Delta m_{\text{atm}}^2 = 2.5 \times 10^{-3} \text{ eV}^2$, assuming this to be the “true” value. Similar results for $\Delta m_{\text{atm}}^2 = 2.0 \times 10^{-3} \text{ eV}^2$ and the same three values of $\sin^2 \theta$ are presented in Fig. 12. We take a systematic uncertainty of 2% and consider 0.1 MeV bins spanning the entire visible energy spectrum between (1.0 – 7.2) MeV. In these figures we keep Δm_{\odot}^2 and $\sin^2 \theta_{\odot}$ fixed at $1.5 \times 10^{-4} \text{ eV}^2$ and 0.3 respectively. Since, as we have shown in the previous Section, the intermediate baseline experiment itself will restrict the allowed values of Δm_{\odot}^2 and $\sin^2 \theta_{\odot}$ to within a few percent of their “true” value, our results remain practically unchanged even if these parameters were allowed to vary freely in the analysis. As Fig. 11 demonstrates, in the 15 (75) GWkTy case the experiment under discussion has almost no sensitivity to the value of Δm_{atm}^2 if $\sin^2 \theta \lesssim 0.02$ (0.01). Note the similarity between these limiting values of $\sin^2 \theta$ and the limit on $\sin^2 \theta$ which the 15 (75) GWkTy experiment can provide if the “true” value of $\sin^2 \theta$ is 0, given in the previous sub-section. This implies that below the indicated respective limiting values of $\sin^2 \theta$, the experiment we are discussing cannot distinguish between a zero and a non-zero $\sin^2 \theta$ and thus fails to “see” the Δm_{atm}^2 –driven oscillations. The reason for the modest sensitivity to $\sin^2 \theta$ is related to the fact that the L is chosen for “our” experiment to be sensitive to the SPMIN due to the Δm_{\odot}^2 –driven oscillations. Correspondingly, L is much bigger than the L^* (cf. Eq. (25)), suitable for the SPMIN associated with the Δm_{atm}^2 –driven oscillations. The lack of accuracy in the reconstruction of the details of a single oscillation period (in E_{vis}) affects strongly the sensitivity to $\sin^2 \theta$ which controls the amplitude of the oscillations. However, this should not affect the sensitivity to Δm_{atm}^2 , which determines the oscillation length, because of the presence of many oscillation periods in the relatively large energy window offered by the spectrum itself.

Thus, if $\sin^2 \theta$ is large enough so that the Δm_{atm}^2 –driven oscillations can be observed in the experiment under discussion, Δm_{atm}^2 can be measured with a high precision. Indeed, in the case when the “true” value of $\sin^2 \theta = 0.03$, Δm_{atm}^2 can be determined to a within few percent accuracy at the 99% C.L. This accuracy could be comparable to the sensitivity of the JPARC (JHF-SK) project to Δm_{atm}^2 ⁹ [43]. It is certainly much better than the sensitivity to Δm_{atm}^2 of the $L = 1.7 \text{ km}$ short baseline experiments [41] with the same statistics. This is somewhat unexpected since the $L = 1.7 \text{ km}$ experiment is optimized to see the Δm_{atm}^2 –driven oscillations. However, one should keep in mind that the $L = 1.7 \text{ km}$ baseline experiment cannot constrain the solar neutrino oscillation parameters. The uncertainty in Δm_{\odot}^2 ¹⁰ allows Δm_{\odot}^2 to take on values as high as $(2 - 3) \times 10^{-4} \text{ eV}^2$. This drastically reduces the sensitivity of the

⁹ The experiment we are discussing has a much larger statistics than the planned JPARC (JHF-SK) experiment; for the precise determination of Δm_{atm}^2 it also requires $\sin^2 \theta$ to be sufficiently large.

¹⁰ For this uncertainty the authors of [41] have used the current 3σ uncertainty on Δm_{\odot}^2 , found in the combined solar neutrino and KamLAND data analysis.

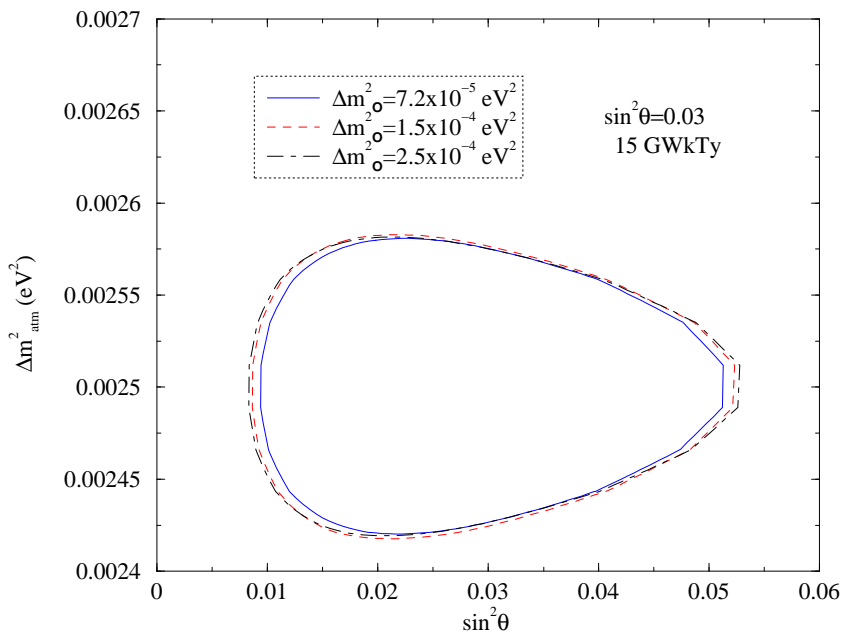


FIG. 13: The impact of the “true” value of Δm_{\odot}^2 on the 99.73% allowed areas when the “true” $\Delta m_{\text{atm}}^2 = 2.5 \times 10^{-3} \text{ eV}^2$ and $\sin^2 \theta = 0.03$.

$L = 1.7 \text{ km}$ experiment to Δm_{atm}^2 . In the experimental set-up we are discussing, the solar parameters are determined to a very high degree of accuracy by the experiment itself and no external input on their errors is required. Thus, the intermediate baseline experiment has a better sensitivity to Δm_{atm}^2 , provided $\sin^2 \theta$ is sufficiently large, while the sensitivity to $\sin^2 \theta$ of the shorter baseline experiment is better for the reasons discussed above, *viz.* it is optimized to the Δm_{atm}^2 -driven SPMIN.

Finally, we show in Fig. 13 the impact of the “true” value of Δm_{\odot}^2 on the ability of the experiment under consideration to measure Δm_{atm}^2 and $\sin^2 \theta$. The figure very clearly demonstrates that even if the low-LMA solution is confirmed as the true solution of the solar neutrino problem, the intermediate baseline experiment could still be used to measure Δm_{atm}^2 and/or constrain $\sin^2 \theta$.

We stress that Figs. 11, 12 and 13 are obtained using Eq. (9), *i.e.*, assuming that the neutrino mass spectrum conforms to a NH. Our conclusions for the sensitivity to $\sin^2 \theta$ and Δm_{atm}^2 would remain the same for the case of IH mass spectrum. For a given “data” set, the allowed region in the parameter space, especially the fitted values of Δm_{atm}^2 , depend on the hierarchy assumed if the Δm_{\odot}^2 is in the high-LMA region. The possibility of two types of neutrino mass hierarchy leads to an ambiguity in the allowed values of Δm_{atm}^2 obtained, as we will show in the next sub-section. However, even though the assumption of the “wrong” hierarchy can lead to another (separated) allowed region in the parameter space, it does not describe the data so well as the “correct” hierarchy and is disfavored, in general. This can be used to gain insight into the type of hierarchy the neutrino mass spectrum has and can allow “our” intermediate baseline experiment to determine the hierarchy.

Let us stress that the question of the hierarchy becomes relevant if Δm_{\odot}^2 lies in the high-LMA zone. This will be the subject of our discussion in the next subsection. If the true solution turns out to be low-LMA, the last terms in Eq. (9) and Eq. (10) would be negligible and sensitivity to hierarchy would be lost. Let us emphasize, however, that even in this case it would still be possible to improve the existing limits on $\sin^2 \theta$, and – if $\sin^2 \theta$ is sufficiently large – to measure Δm_{atm}^2 with an exceptional precision.

C. Normal vs. Inverted Hierarchy

The next question that may be answered with the experiment under discussion is whether the neutrino mass spectrum is with normal hierarchy or with inverted hierarchy. As pointed out in Section III and follows from Eq. (21), the baseline $L = 20 \div 30 \text{ km}$ is particularly suited for that purpose. In this subsection we present results for $L = 20 \text{ km}$. We use the highest statistics and smallest energy bins and consider the entire visible energy spectrum with a

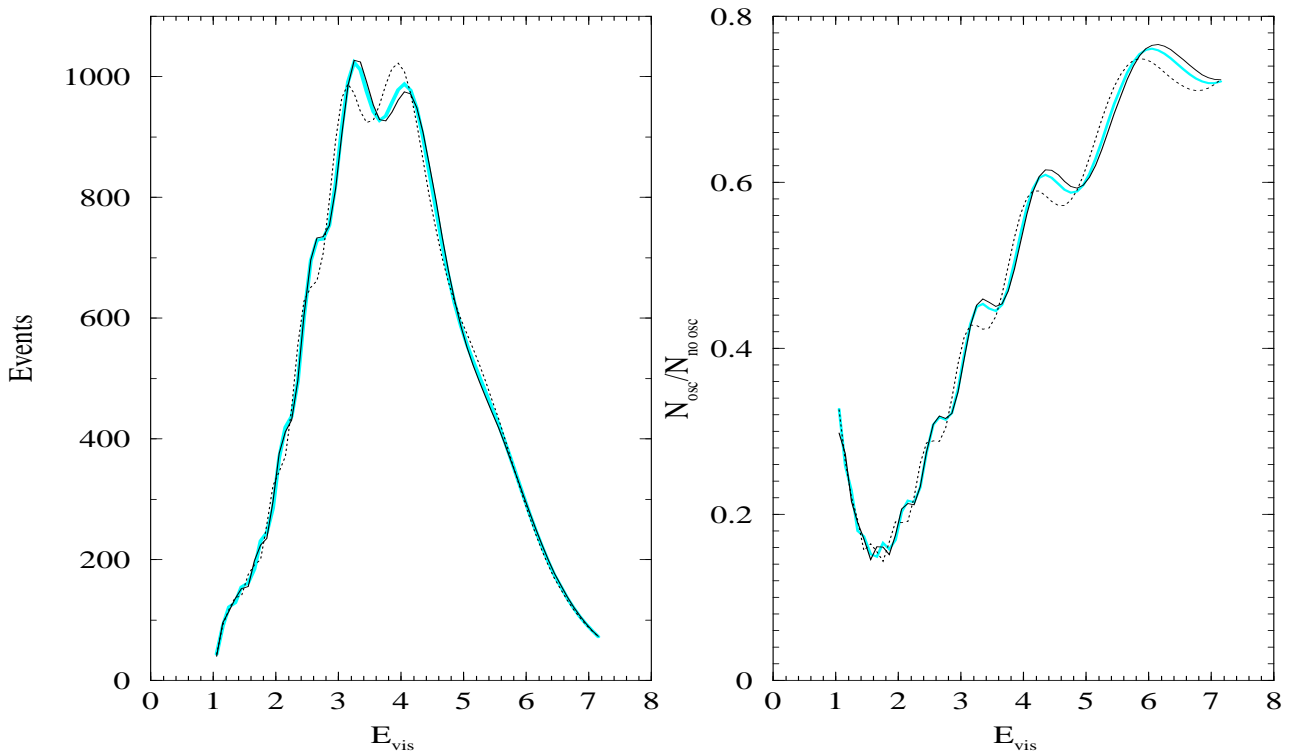


FIG. 14: The energy spectrum (in 0.1 MeV bins) of the events in the case of $\bar{\nu}_e$ oscillations (left-panel), and the ratio of events in the cases of oscillations and absence of oscillations (right-panel), showing the effect of hierarchy for a $L = 20$ km experiment. The thick cyan/grey line corresponds to the case for NH with $\Delta m_{\text{atm}}^2 = 2.5 \times 10^{-3} \text{ eV}^2$ while the dotted and thin solid line correspond to the case of IH with $\Delta m_{\text{atm}}^2 = 2.5 \times 10^{-3} \text{ eV}^2$ and $\Delta m_{\text{atm}}^2 = 2.6 \times 10^{-3} \text{ eV}^2$, respectively. The statistics assumed is $\mathcal{L} = 75 \text{ GWkTy}$, while $\sin^2 \theta = 0.03$, $\Delta m_{\odot}^2 = 1.5 \times 10^{-4} \text{ eV}^2$ and $\sin^2 \theta_{\odot} = 0.3$.

low energy cut-off of $E_{th} = 1.0$ MeV. We assume also that the “true” value of $\sin^2 \theta$ is non-zero and is sufficiently large. As it follows from Eq. (9) and Eq. (10), the predictions for the final state e^+ -spectrum distortions in the NH and IH cases differ only if the solar neutrino mixing angle $\theta_{\odot} \neq \pi/4$. Maximal mixing is currently disfavored by the solar neutrino and KamLAND data [11, 12, 13]. We use the current best-fit value for the solar neutrino mixing angle, corresponding to $\sin^2 \theta_{\odot} = 0.3$. The value of $\sin^2 \theta_{\odot}$ will be measured with a very high precision in the reactor experiment under discussion itself.

In Fig. 14 we show the visible energy spectrum expected for both the NH and IH cases. The left-hand panel shows the number of events, while the right-hand panel shows the ratio of the number of events in the case of $\bar{\nu}_e$ oscillation (“oscillation events”) to the number of events in the absence of oscillations (“no oscillation events”). The thick cyan/grey line is for the case of $\Delta m_{\text{atm}}^2 = 2.5 \times 10^{-3} \text{ eV}^2$ and NH, the dotted line corresponds to $\Delta m_{\text{atm}}^2 = 2.5 \times 10^{-3} \text{ eV}^2$ and IH, while the thin solid line is for $\Delta m_{\text{atm}}^2 = 2.6 \times 10^{-3} \text{ eV}^2$ and IH. Thus, for the same value of Δm_{atm}^2 , the e^+ -spectrum deformations expected for NH and IH are different owing to the last terms in Eq. (9) and Eq. (10). One might expect on the basis of Eqs. (9) and (10) that the IH e^+ -spectrum would fit a NH e^+ -spectrum with a value of Δm_{atm}^2 that is larger than the “true” value by a range which would be of the order of Δm_{\odot}^2 . If the experiment has a sensitivity to Δm_{atm}^2 which is better than, or is at least of the same order as Δm_{\odot}^2 , one might expect two non-degenerate solutions in the $\Delta m_{\text{atm}}^2 - \sin^2 \theta$ parameter space for the same data set: one for NH and another for IH.

However, we would like to stress that even though the IH e^+ -spectrum could approximately reproduce the NH e^+ -spectrum, it cannot exactly reproduce the latter. Hence, if the NH is the true hierarchy, the case of IH mass spectrum would always be disfavored by the data from “our” experiment compared to the NH spectrum. We have seen in the previous Section that the experimental set-up we are discussing could have a very high sensitivity to Δm_{atm}^2 , and therefore we can expect the large statistics intermediate baseline reactor experiments to determine the type of neutrino mass hierarchy, for sufficiently large $\sin^2 \theta$ at least, if the high-LMA solution holds.

In Fig. 15 we explicitly show the allowed regions obtained using a “data” set generated in the NH case and fitted by both the NH and IH expressions for the $\bar{\nu}_e$ survival probability. The results shown are obtained using the 75

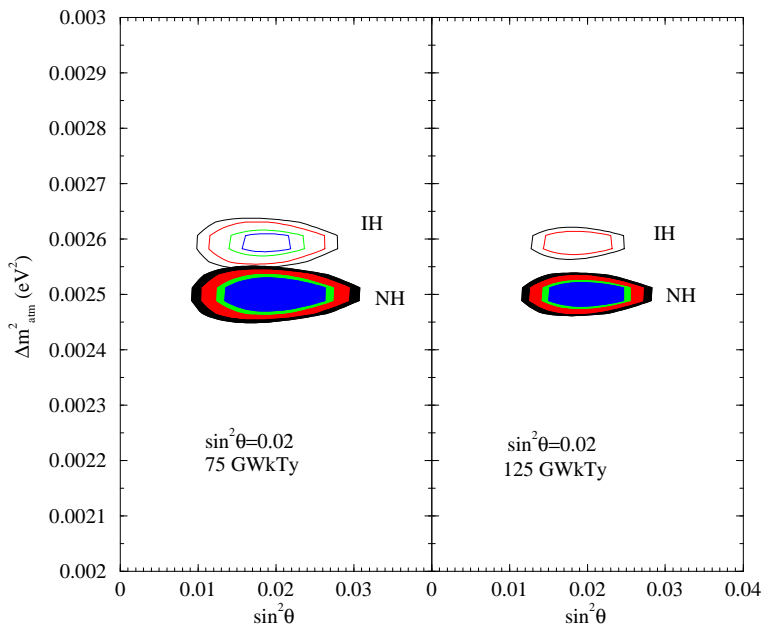


FIG. 15: The same as in Fig. 11, but probing the type of the neutrino mass hierarchy. The “data” sets simulated correspond to NH. The filled contours show the C.L. allowed regions obtained by fitting for the parameters assuming NH. The empty contours show the 90%, 95%, 99% and 99.73% solution regions, obtained by fitting the NH “data” with an IH theory. The contours for the IH are obtained with respect to the χ^2 -minima found in the case of the NH. The statistics assumed in the left-hand panel is $\mathcal{L} = 75$ GWkTy, while that in the right-hand panel is $\mathcal{L} = 125$ GWkTy. We note that while for the $\mathcal{L} = 75$ GWkTy case the “wrong” hierarchy is allowed even at the 90% C.L., with the $\mathcal{L} = 125$ GWkTy statistics the experiment can rule out the IH at least at the 95% C.L.

GWkTy statistics and a higher 125 GWkTy statistics. The “true” value of Δm_{atm}^2 assumed is $2.5 \times 10^{-3} \text{ eV}^2$, while “true” $\sin^2 \theta = 0.02$. For the 75 GWkTy case, the two regions overlap at the 3σ level, while for 125 GWkTy they are completely non-degenerate. Note also that for the 125 GWkTy case, the “data” generated for NH spectrum can “rule out” the IH spectrum, at least at the 95% C.L.

In Fig. 16 we show the dependence of the hierarchy sensitivity of the $L = 20$ km reactor experiment on the “true” values of Δm_{atm}^2 , $\sin^2 \theta$ and Δm_{\odot}^2 . For each point in the $\Delta m_{\text{atm}}^2 - \sin^2 \theta$ parameter space and a given Δm_{\odot}^2 and $\sin^2 \theta_{\odot}$, we simulate the observed e^+ -energy spectrum assuming NH to be true. We then fit this “observed” spectrum with both the NH and IH through a χ^2 analysis, allowing the parameters Δm_{atm}^2 and $\sin^2 \theta$ to vary freely around their “true” values. The IH spectrum obviously does not fit the “data” as well as the NH and hence is disfavored. To quantify this sensitivity to hierarchy we calculate the difference (χ_{diff}^2) between the χ^2 for the NH and IH for each point in the parameter space and use the definition $\chi_{\text{diff}}^2 < \Delta\chi^2$ to find whether IH can be ruled out at a given C.L. The $\Delta\chi^2$ is determined by the C.L. considered and we take the 2-parameter definition for it. We show the lines of the C.L. contours in the $\Delta m_{\text{atm}}^2 - \sin^2 \theta$ plane for 2 different values of Δm_{\odot}^2 and $\sin^2 \theta_{\odot} = 0.3$. All “true” values of the parameters located to the right of a given line, could allow the experiment to disfavor the IH spectrum at the corresponding C.L. The solid lines give the sensitivities for 75 GWkTy exposure, while the dashed lines are for a 125 GWkTy data set. The sensitivity to hierarchy is maximal for the smallest allowed values of Δm_{atm}^2 and for these cases it is possible to rule out IH even for smaller values of $\sin^2 \theta$. It becomes increasingly more difficult to distinguish between the two types of neutrino mass hierarchy as Δm_{atm}^2 increases, as the figure indicates. The sensitivity of the experiment to hierarchy depends critically on the “true” value of the solar parameters, as is evident from Eq. (9) and Eq. (10). In particular, higher values of Δm_{\odot}^2 are better suited for hierarchy determination, as can be seen explicitly comparing the two panels in Fig. 16.

The possibility of determining the neutrino mass hierarchy is very sensitive to the value of $\sin^2 \theta_{\odot}$. As we have explained above, when we generate the NH “data” and fit them with the IH theory, we allow Δm_{atm}^2 to vary and take larger values than Δm_{atm}^2 used to generate the “data”. Let us denote the best-fit Δm_{atm}^2 in the IH case as $\Delta m_{\text{atm}}^{\prime 2}$:

$$\Delta m_{\text{atm}}^{\prime 2} = \Delta m_{\text{atm}}^2 + \Delta m^2, \quad (34)$$

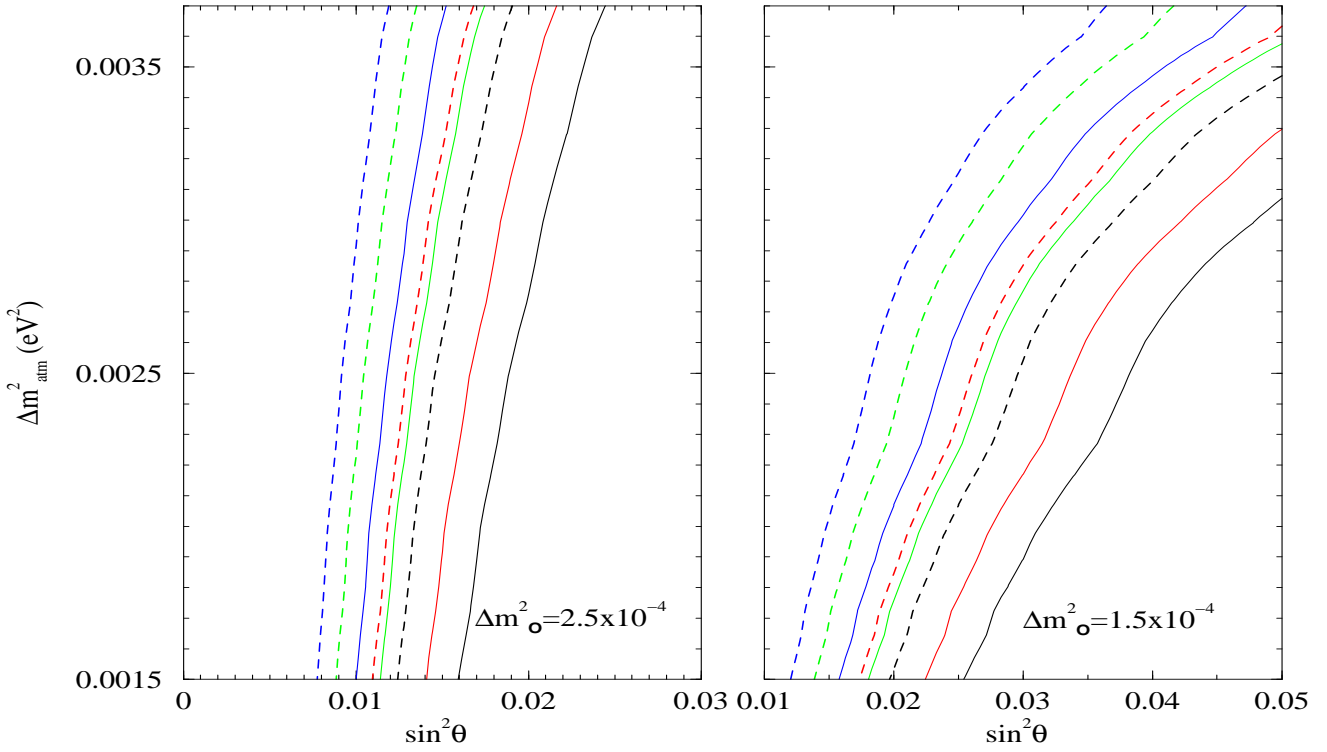


FIG. 16: Contours of constant 99.73%(black), 99%(red), 95%(green) and 90%(blue) C.L., showing the ability of the $L = 20$ km baseline experiment to determine the correct hierarchy at each “true” point in the $\Delta m_{\text{atm}}^2 - \sin^2 \theta$ plane. The solid lines (dashed lines) correspond to $\mathcal{L} = 75$ GWkTy ($\mathcal{L} = 125$ GWkTy). The results shown are for $\sin^2 \theta_{\odot} = 0.30$, and for $\Delta m_{\odot}^2 = 1.5 \times 10^{-4}$ eV² (right panel) and $\Delta m_{\odot}^2 = 2.5 \times 10^{-4}$ eV² (left panel). For the values of Δm_{atm}^2 and $\sin^2 \theta$, corresponding to points on the plane, located to the right of a given C.L. line, the experiment can rule out the “wrong” hierarchy at that C.L. See the text for further details.

where $\Delta m^2 > 0$. The difference between the IH and NH $\bar{\nu}_e$ survival probabilities at each E is given by:

$$\begin{aligned}
P_{IH}(\bar{\nu}_e \rightarrow \bar{\nu}_e) - P_{NH}(\bar{\nu}_e \rightarrow \bar{\nu}_e) = & 4 \sin^2 \theta \cos^2 \theta \left[\sin\left(\frac{\Delta m_{\text{atm}}^2 L}{2E} + \frac{\Delta m^2 L}{4E}\right) \sin\left(-\frac{\Delta m^2 L}{4E}\right) \right. \\
& + \cos^2 \theta_{\odot} \sin\left(\frac{\Delta m_{\text{atm}}^2 L}{2E} + \frac{\Delta m^2 L}{2E} - \frac{\Delta m_{\odot}^2 L}{4E}\right) \sin\left(\frac{\Delta m_{\odot}^2 L}{4E}\right) \\
& \left. - \sin^2 \theta_{\odot} \sin\left(\frac{\Delta m_{\text{atm}}^2 L}{2E} - \frac{\Delta m_{\odot}^2 L}{4E}\right) \sin\left(\frac{\Delta m_{\odot}^2 L}{4E}\right) \right] \quad (35)
\end{aligned}$$

When, e.g., $\cos 2\theta_{\odot} = 1$, we have $P_{IH} - P_{NH} = 0$ for $\Delta m^2 = \Delta m_{\odot}^2$. For $\cos 2\theta_{\odot} = 0$ (maximal mixing), the difference between the two probabilities is 0 for $\Delta m^2 = 0$. For the realistic case of $\cos 2\theta_{\odot} \cong (0.10 - 0.40)$, it is impossible to have $P_{IH} - P_{NH} = 0$ for every value of E from the interval of interest. This is illustrated in Fig. 17, where we show the difference between the minimal values of χ^2 for the “wrong” IH and the “right” NH spectra as a function of $\sin^2 \theta_{\odot}$ for “true” $\Delta m_{\odot}^2 = 1.5 \times 10^{-4}$; 2.5×10^{-4} ; 3.5×10^{-4} eV², $\Delta m_{\text{atm}}^2 = 2.5 \times 10^{-3}$ eV² and $\sin^2 \theta = 0.03$. As Fig. 17 indicates, the best sensitivity to the type of neutrino mass hierarchy is achieved in the interval $\sin^2 \theta_{\odot} \cong (0.3 - 0.45)$, which is favored by the current solar neutrino and KamLAND data. The rather strong dependence of the sensitivity to the type of neutrino mass hierarchy on $\sin^2 \theta_{\odot}$ is illustrated in Fig. 18, in which we show contours of constant C.L. in the $\Delta m_{\text{atm}}^2 - \sin^2 \theta$ plane, at which one could distinguish between the NH and IH spectra, for $\Delta m_{\odot}^2 = 3.5 \times 10^{-4}$ eV² and $\sin^2 \theta_{\odot} = 0.30$; 0.40.

One final comment is in order. As Fig. 15 illustrates, for a given “data set” (i.e., “true” value of Δm_{atm}^2 , etc.) and sufficient statistics, the neutrino mass hierarchy ambiguity can lead to two non-degenerate solutions for Δm_{atm}^2 , one for NH and another for IH spectrum. In certain of these cases the intermediate baseline reactor experiment might not be able to rule out the “wrong” hierarchy even at the 90% C.L. (Fig. 15, left panel). However, since the NH and IH give two different and non-degenerate values for Δm_{atm}^2 , in such cases one can use the information from some other

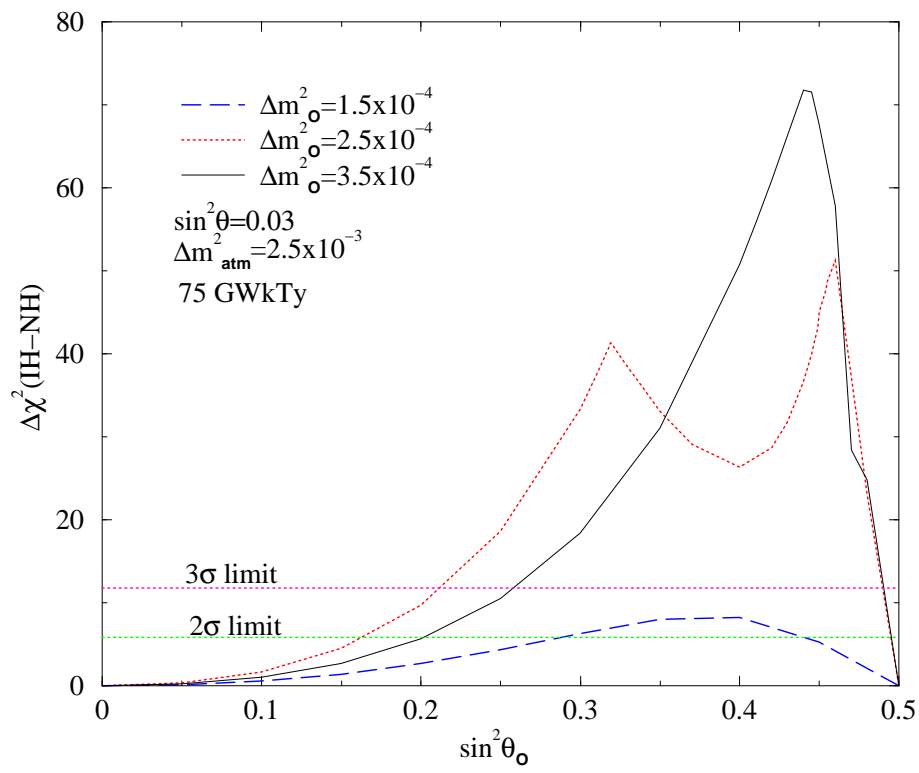


FIG. 17: The difference between the minimal values of χ^2 , obtained by fitting a NH “data” set with NH and IH spectrum, as a function of $\sin^2\theta_\odot$. The results shown are for $\Delta m_\odot^2 = 1.5 \times 10^{-3}$; 2.5×10^{-3} ; 3.5×10^{-3} eV². The “true” values of $\Delta m_{\text{atm}}^2 = 2.5 \times 10^{-3}$ eV² and of $\sin^2\theta = 0.03$, while the statistics corresponds to $\mathcal{L} = 75$ GWkTy.

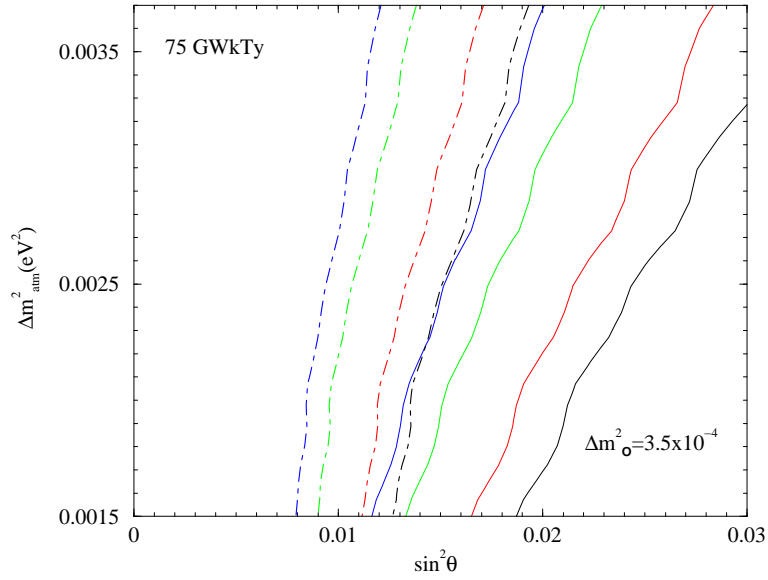


FIG. 18: The same as in Fig. 16, for $\mathcal{L} = 75$ GWkTy, $\Delta m_\odot^2 = 3.5 \times 10^{-4}$ eV² and two values of $\sin^2\theta_\odot$: 0.30 (solid lines) and 0.40 (dash-dotted lines).

very precise experiment, like the proposed JHF-SK or NuMI off-axis experiments with neutrino superbeams [43, 44], to determine the correct value of Δm_{atm}^2 . The latter can be used together with the data from the reactor experiment to get information on the hierarchy.

VI. CONCLUSIONS

In this paper we analyzed the physics potential of a reactor neutrino experiment with a relatively large detector at a distance $L \sim 20 \div 30$ km. This distance has been chosen in order to achieve the best sensitivity to the solar neutrino oscillation parameters Δm_{\odot}^2 and $\sin^2 \theta_{\odot}$, assuming that the latter lie in the high-LMA solution region. We considered the case of three flavor neutrino mixing and used in the analysis the exact expression for the relevant $\bar{\nu}_e$ survival probability. The latter depends, in addition to Δm_{\odot}^2 and $\sin^2 \theta_{\odot}$, on Δm_{atm}^2 , driving the atmospheric neutrino oscillations, on θ – the angle limited by the CHOOZ and Palo Verde experiments, and for $\sin^2 \theta_{\odot} < 0.50$ – on the type of the neutrino mass spectrum which can be with normal hierarchy (NH) or with inverted hierarchy (IH). The current solar neutrino and KamLAND data favor $\sin^2 \theta_{\odot} \sim 0.30$. We discussed strategies and the experimental set-up, which would permit to measure Δm_{\odot}^2 and $\sin^2 \theta_{\odot}$ with a high precision, get information on (or even measure) $\sin^2 \theta$, and if $\sin^2 \theta$ is sufficiently large ($\sin^2 \theta \gtrsim 0.02$) provide a high precision measurement of Δm_{atm}^2 and determine the type of the neutrino mass hierarchy. More specifically, we have investigated the impact that i) the choice of the baseline L , ii) the effect of using a relatively low e^+ –energy cut-off of $E_{th} \sim 1.0$ MeV, iii) the detector’s energy resolution, as well as iv) the statistical and systematical errors, can have on the measurement of each of the indicated neutrino oscillation parameters.

The precision with which Δm_{\odot}^2 and $\sin^2 \theta_{\odot}$ can be determined in the experiment under discussion depends crucially on whether the first Δm_{\odot}^2 –driven oscillation minimum of the $\bar{\nu}_e$ survival probability falls or not in the interval of e^+ –energies which can be used for the measurements in the experiment. For $\Delta m_{\odot}^2 = 1.5 \times 10^{-4}$ eV² (2.5×10^{-4} eV²) and $L = 20$ km, this minimum takes place at the e^+ –energy of $E_{vis} = 1.6$ (3.2) MeV; for $L = 30$ km, it occurs at $E_{vis} = 2.8$ (5.3) MeV. This implies that if $\Delta m_{\odot}^2 = 1.5 \times 10^{-4}$ eV², in order to achieve a high precision in the determination of Δm_{\odot}^2 and especially of $\sin^2 \theta_{\odot}$ in an experiment with a baseline of $L = 20$ km, a relatively low “threshold” energy should be employed, $E_{th} \sim 1.0$ MeV. If, however, $\Delta m_{\odot}^2 \gtrsim 2.0 \times 10^{-4}$ eV², one can use $E_{th} \cong 2.6$ MeV, as was done in the KamLAND experiment. In the case of $L = 30$ km one can use $E_{th} \cong 2.6$ MeV even for $\Delta m_{\odot}^2 \gtrsim 1.5 \times 10^{-4}$ eV². If the condition under discussion is fulfilled, remarkable precision in the measurement of Δm_{\odot}^2 and $\sin^2 \theta$ can be achieved. For the lower “threshold” energy, $E_{th} \sim 1.0$ MeV, achieving high precision requires a controllable or negligible background due to the geophysical neutrinos in the interval $E_{vis} = (1.0 - 2.6)$ MeV. If a sufficiently accurate modeling of this background is achieved and $E_{th} = 1.0$ MeV, assuming $\Delta m_{\odot}^2 = 1.5 \times 10^{-4}$ eV², energy bins of $\Delta E = 0.425$ MeV, $\sin^2 \theta_{\odot} = 0.3$, 2% systematic error and a total statistics corresponding to $\mathcal{L} = 15$ GWkTy, one could determine Δm_{\odot}^2 with up to a $\sim 2\%$, and $\sin^2 \theta_{\odot}$ with a $3 \div 4\%$ uncertainty at 99% C.L. in an experiment with a baseline of $L = 20$ km (Figs. 3 - 5). This impressive results depend rather mildly on the systematic error provided the latter does not exceed $\sim 4\%$ (Fig. 7). The reduction of the e^+ –energy bin width leads to a negligible change in the precision with which Δm_{\odot}^2 and $\sin^2 \theta_{\odot}$ are measured (Fig. 6). The precision can be even higher in the case of a larger statistics (e.g., for $\mathcal{L} = 75$ GWkTy, Fig. 8).

The same apparatus could be used to extract information on the other parameters entering into the expression for the survival probability, through the study of sub-leading effects controlled by the (small) mixing angle θ , for which only upper bounds exist at present.

The limit on $\sin^2 \theta$ can be lowered to $\sin^2 \theta < 0.021$ at 99.73% C.L. for $L = 20$ km, if the “threshold” energy $E_{th} = 1.0$ MeV, the systematic error is 2%, the e^+ –energy bin width is $\Delta E = 0.1$ MeV and if statistics corresponding to $\mathcal{L} = 15$ GWkTy is collected. This result depends strongly on the choice of L : the optimal distance for such a measurement is of a few km, and the shorter the distance with respect to $L = 20$ km the stronger this bound would be. The magnitude of e^+ –energy bin width and the value of the e^+ –energy effective threshold have a considerable impact on the bound as well, while a further reduction of the systematic errors could lead only to a mild improvement. If the statistics is as large as that corresponding to a set up with $\mathcal{L} = 75$ GWkTy, one could improve the upper bound to $\sin^2 \theta < 0.010$ (0.0055) at 99.73% (90%) C.L.

If, on the contrary, a relatively large non-vanishing value of $\sin^2 \theta$ is found, the experiment could gain sensitivity to Δm_{atm}^2 through the detection of the sub-leading oscillatory properties of the $\bar{\nu}_e$ survival probability. Not averaging out the Δm_{atm}^2 –driven oscillations is crucial for the measurement of Δm_{atm}^2 . This requires a relatively high e^+ –energy resolution, permitting a binning in the e^+ –energy with a rather small bin width, $\Delta E \cong 0.1$ MeV. Taking $E_{th} = 1.0$ MeV and assuming 2% systematic error, we find that a set-up with $\mathcal{L} = 15$ (75) GWkTy could provide a precise determination of Δm_{atm}^2 with a few percent uncertainty for $\Delta m_{\text{atm}}^2 \sim 2.5 \times 10^{-3}$ eV², if $\sin^2 \theta \sim 0.03$ (0.02) (Fig. 11).

Finally, the distance $L = 20$ km is the optimal one for distinguishing between the NH and IH neutrino mass

spectrum. The relevant $\bar{\nu}_e$ survival probabilities for the two types of spectrum differ for $\sin^2 \theta_\odot < 0.5$ by a $\sin^2 \theta$ -suppressed interference term due to the amplitudes of the Δm_\odot^2 - and Δm_{atm}^2 - driven oscillations. For this highly challenging study, a very large statistics is necessary: we considered $\mathcal{L} = 75$ and 125 GWkTy. The possibility of distinguishing between the two types of neutrino mass hierarchy was found to depend not only on the values of $\sin^2 \theta$ and $\sin^2 \theta_\odot$, but also on the values of Δm_\odot^2 and Δm_{atm}^2 . The dependence on Δm_\odot^2 and $\sin^2 \theta_\odot$ is particularly strong. For $\Delta m_\odot^2 = 1.5 \times 10^{-4} \text{ eV}^2$, and $\mathcal{L} = 75$ (125) GWkTy, one could distinguish the NH from the IH spectrum at 99.73% C.L. in the region of $\Delta m_{\text{atm}}^2 \lesssim 2.5 \times 10^{-3} \text{ eV}^2$ if $\sin^2 \theta \gtrsim 0.038$ (0.03) (Fig. 16). The type of the neutrino mass spectrum can be determined for considerably smaller values of $\sin^2 \theta$ if Δm_\odot^2 has a larger value (Figs. 17 and 18), or if an even larger statistics would be accumulated. For $\mathcal{L} = 75$ GWkTy and $\Delta m_\odot^2 = 2.5 \times 10^{-4} \text{ eV}^2$, for instance, this can be done at 99.73% C.L. for $\sin^2 \theta \gtrsim 0.019$ if $\Delta m_{\text{atm}}^2 \lesssim 2.5 \times 10^{-3} \text{ eV}^2$ and $\sin^2 \theta_\odot = 0.30$ (Fig. 16). As we have shown, the highest sensitivity to the type of the neutrino mass hierarchy is achieved for $\sin^2 \theta_\odot \cong (0.30 - 0.45)$ (Figs. 17 and 18).

To conclude, the intermediate baseline $L \cong 20$ km reactor neutrino experiments have in the case of the high-LMA solution of the solar neutrino problem a remarkable potential for a high precision measurement of the solar neutrino oscillation parameters Δm_\odot^2 and $\sin^2 \theta_\odot$, which can reduce the error in the values of the latter to a (2 – 4)%. Such an experiment can also improve the existing bounds on, or measure, $\sin^2 \theta$, currently limited by the CHOOZ and Palo Verde data. If $\sin^2 \theta$ turns out to be relatively large, $\sin^2 \theta \gtrsim 0.02$, the same experiment could measure Δm_{atm}^2 , driving the atmospheric neutrino oscillations, with an error of a few percent and might be able to establish whether the neutrino mass spectrum is with normal or inverted hierarchy.

Acknowledgements.

S.T.P. would like to thank T. Lasserre for useful discussions and the members of APC Institute at College de France, Paris, and the organizers of the Program on “Neutrinos: Data, Cosmos and the Planck Scale” at KITP, Univ. of California at Santa Barbara, where parts of the work on the present study were done, for kind hospitality. M.P. would like to thank R. Shrock and R.G.H. Robertson for useful discussions. S.C. acknowledges help from S. Goswami and A. Bandyopadhyay in developing the computer code used for numerical calculations in the present work, and would like to thank F. Suekane for useful correspondence. This work was supported in part by the Italian MIUR and INFN under the programs “Fenomenologia delle Interazioni Fondamentali” and “Fisica Astroparticellare” (S.T.P. and S.C.), by the U.S. National Science Foundation under Grant No. PHY99-07949 (S.T.P.) and by the US Department of Energy under contract DE-FG02-92ER-40704 (M.P.).

-
- [1] B. T. Cleveland *et al.*, *Astrophys. J.* **496**, 505 (1998);
J. N. Abdurashitov *et al.* [SAGE Collaboration], arXiv:astro-ph/0204245;
W. Hampel *et al.* [GALLEX Collaboration], *Phys. Lett. B* **447**, 127 (1999);
E. Bellotti, Talk at Gran Sasso National Laboratories, Italy, May 17, 2002; T. Kirsten, talk at *Neutrino 2002*, XXth International Conference on Neutrino Physics and Astrophysics, Munich, Germany, May 25-30, 2002. (<http://neutrino2002.ph.tum.de/>)
 - [2] S. Fukuda *et al.* [Super-Kamiokande Collaboration], of Super-Kamiokande solar neutrino data,” *Phys. Rev. Lett.* **86**, 5656 (2001) [arXiv:hep-ex/0103033]; S. Fukuda *et al.* [Super-Kamiokande Collaboration], *Phys. Rev. Lett.* **86**, 5651 (2001) [arXiv:hep-ex/0103032].
 - [3] Q. R. Ahmad *et al.* [SNO Collaboration], *Phys. Rev. Lett.* **87**, 071301 (2001) [arXiv:nucl-ex/0106015]; Q. R. Ahmad *et al.* [SNO Collaboration], *Phys. Rev. Lett.* **89**, 011301 (2002) [arXiv:nucl-ex/0204008].
 - [4] Y. Fukuda *et al.* [Super-Kamiokande Collaboration], *Phys. Rev. Lett.* **81**, 1562 (1998) [arXiv:hep-ex/9807003]; M. Shiozawa, talk given at the Int. Conf. on Neutrino Physics and Astrophysics “Neutrino’02”, May 25 - 30, 2002, Munich, Germany.
 - [5] M. H. Ahn *et al.* [K2K Collaboration], *Phys. Rev. Lett.* **90**, 041801 (2003) [arXiv:hep-ex/0212007].
 - [6] K. Eguchi *et al.* [KamLAND Collaboration], *Phys. Rev. Lett.* **90**, 021802 (2003) [arXiv:hep-ex/0212021].
 - [7] B. Pontecorvo, *Zh. Eksp. Teor. Fiz.* **53**, 1717 (1967) [*Sov. Phys. JETP* **26**, 984 (1968)]; S. M. Bilenky and B. Pontecorvo, *Phys. Rep.* **41**, 225 (1978).
 - [8] S.M. Bilenky and S.T. Petcov, *Rev. Mod. Phys.* **59** (1987) 671.
 - [9] S.T. Petcov, *Lecture Notes in Physics*, v. 512 (eds. H. Gausterer and C.B. Lang, Springer, 1998), p. 281. (hep-ph/9806466).
 - [10] S. Choubey *et al.*, arXiv:hep-ph/0209222; A. Bandyopadhyay *et al.*, *Phys. Lett. B* **540**, 14 (2002) [arXiv:hep-ph/0204286].

- [11] G. L. Fogli et al., Phys. Rev. D **67**, 073002 (2003) [arXiv:hep-ph/0212127];
- [12] A. Bandyopadhyay et al., Phys. Lett. B **559**, 121 (2003) [arXiv:hep-ph/0212146];
- [13] M. Maltoni, T. Schwetz and J. W. Valle, arXiv:hep-ph/0212129; J. N. Bahcall, M. C. Gonzalez-Garcia and C. Pena-Garay, JHEP **0302**, 009 (2003) [arXiv:hep-ph/0212147]; H. Nunokawa, W. J. Teves and R. Zukanovich Funchal, arXiv:hep-ph/0212202; P. Aliani et al., arXiv:hep-ph/0212212; P. C. de Holanda and A. Y. Smirnov, JCAP **0302**, 001 (2003) [arXiv:hep-ph/0212270].
- [14] G. L. Fogli et al., arXiv:hep-ph/0303064.
- [15] S. M. Bilenky, C. Giunti and W. Grimus, Prog. Part. Nucl. Phys. **43** (1999) 1 (hep-ph/9812360).
- [16] B. Pontecorvo, Zh. Eksp. Teor. Fiz. **33** (1957) 549, and **34** (1958) 247.
- [17] Z. Maki, M. Nakagawa and S. Sakata, Prog. Theor. Phys. **28** (1962) 870.
- [18] S.M. Bilenky et al., Phys. Lett. **B94** (1980) 495.
- [19] M. Doi et al., Phys. Lett. **B102** (1981) 323.
- [20] P. Langacker et al., Nucl.Phys. **B282** (1987) 589.
- [21] M. Apollonio et al. [CHOOZ Collaboration], Phys. Lett. **B466** (1999) 415 (hep-ex/9907037).
- [22] F. Boehm, J. Busenitz et al., Phys. Rev. Lett. **84** (2000) 3764 and Phys. Rev. **D62** (2000) 072002.
- [23] S. M. Bilenky, D. Nicolo and S. T. Petcov, Phys. Lett. B **538**, 77 (2002) [arXiv:hep-ph/0112216].
- [24] A. De Rujula et al., Nucl. Phys. **B168** (1980) 54.
- [25] S. M. Bilenky et al., Phys. Lett. B **356**, 273 (1995) [arXiv:hep-ph/9504405];
- [26] D. Michael (MINOS Collaboration), Talk at the Int. Conf. on Neutrino Physics and Astrophysics “Neutrino’02”, May 25 - 30, 2002, Munich, Germany.
- [27] M. Spiro, Summary talk at the Int. Conf. on Neutrino Physics and Astrophysics “Neutrino’02”, May 25 - 30, 2002, Munich, Germany.
- [28] A. Bandyopadhyay et al., arXiv:hep-ph/0211266; V. D. Barger, D. Marfatia and B. P. Wood, Phys. Lett. B **498**, 53 (2001) [arXiv:hep-ph/0011251]; H. Murayama and A. Pierce, Phys. Rev. D **65**, 013012 (2002) [arXiv:hep-ph/0012075].
- [29] A. Bandyopadhyay, S. Choubey and S. Goswami, arXiv:hep-ph/0302243.
- [30] S. T. Petcov and M. Piai, Phys. Lett. B **533**, 94 (2002) [arXiv:hep-ph/0112074].
- [31] S. Schonert, T. Lasserre and L. Oberauer, Astropart. Phys. **18**, 565 (2003) [arXiv:hep-ex/0203013].
- [32] S.M. Bilenky et al., Phys. Lett. **B465** (1999) 193; S.M. Bilenky, S. Pascoli and S.T. Petcov, Phys. Rev. **D64** (2001) 053010; S. Pascoli and S.T. Petcov, Phys. Lett. **B544** (2002) 239; S. Pascoli, S.T. Petcov and W. Rodejohann, Phys. Lett. **B558** (2003) 141.
- [33] M. Freund et al., Nucl. Phys. **B578** (2000) 27; see also, e.g., A. De Rujula, M.B. Gavela and P. Hernandez, Nucl. Phys. **B547**, 21 (1999), and V. Barger et al., Phys. Rev. **D62**, 013004 (2000).
- [34] V. Barger, D. Marfatia and K. Whisnant, hep-ph/0210428; P. Huber, M. Lindner and W. Winter, hep-ph/0211300.
- [35] A. Bandyopadhyay, S. Choubey, S. Goswami and K. Kar, Phys. Rev. D **65**, 073031 (2002) [arXiv:hep-ph/0110307].
- [36] S.M. Bilenky et al., Phys. Rev. D **54** (1996) 4432 (hep-ph/9604364).
- [37] V. I. Kopeikin, L. A. Mikaelyan and V. V. Sinev, Phys. Atom. Nucl. **64**, 849 (2001) [Yad. Fiz. **64**, 914 (2001)] (hep-ph/0110290).
- [38] G. Fiorentini et al., Phys. Lett. B **558**, 15 (2003) [arXiv:hep-ph/0301042].
- [39] C. Bemporad, G. Gratta and P. Vogel, Rev. Mod. Phys. **74**, 297 (2002) [arXiv:hep-ph/0107277].
- [40] M. C. Gonzalez-Garcia and C. Pena-Garay, Phys. Lett. B **527**, 199 (2002) [arXiv:hep-ph/0111432].
- [41] P. Huber et al., arXiv:hep-ph/0303232.
- [42] H. Minakata et al., arXiv:hep-ph/0211111.
- [43] Y. Itow et al., arXiv:hep-ex/0106019
- [44] D. Ayres et al., arXiv:hep-ex/0210005.